



---

MSU Graduate Theses

---

Summer 2021

## Investigation of the Interface Reactions of Ion Selective Electrode Membranes Using Chromatographic and Spectroscopic Analyses of Erbium(III) Tetraphenylporphyrin

Alexis Rae Miller

Missouri State University, al127@live.missouristate.edu

As with any intellectual project, the content and views expressed in this thesis may be considered objectionable by some readers. However, this student-scholar's work has been judged to have academic value by the student's thesis committee members trained in the discipline. The content and views expressed in this thesis are those of the student-scholar and are not endorsed by Missouri State University, its Graduate College, or its employees.

---

Follow this and additional works at: <https://bearworks.missouristate.edu/theses>

 Part of the [Analytical Chemistry Commons](#)

### Recommended Citation

Miller, Alexis Rae, "Investigation of the Interface Reactions of Ion Selective Electrode Membranes Using Chromatographic and Spectroscopic Analyses of Erbium(III) Tetraphenylporphyrin" (2021). *MSU Graduate Theses*. 3651.

<https://bearworks.missouristate.edu/theses/3651>

This article or document was made available through BearWorks, the institutional repository of Missouri State University. The work contained in it may be protected by copyright and require permission of the copyright holder for reuse or redistribution.

For more information, please contact [BearWorks@library.missouristate.edu](mailto:BearWorks@library.missouristate.edu).

**INVESTIGATION OF THE INTERFACE REACTIONS OF ION SELECTIVE  
ELECTRODE MEMBRANES USING CHROMATOGRAPHIC AND  
SPECTROSCOPIC ANALYSES OF ERBIUM(III)  
TETRAPHENYLPORPHYRIN**

A Master's Thesis

Presented to

The Graduate College of

Missouri State University

In Partial Fulfillment

Of the Requirements for the Degree

Master of Science, Chemistry

By

Alexis Rae Miller

July 2021

Copyright 2021 by Alexis Rae Miller

**INVESTIGATION OF THE INTERFACE REACTIONS OF ION SELECTIVE  
ELECTRODE MEMBRANES USING CHROMATOGRAPHIC AND SPECTROSCOPIC  
ANALYSES OF ERBIUM(III) TETRAPHENYLPORPHYRIN**

Chemistry

Missouri State University, July 2021

Master of Science

Alexis Rae Miller

**ABSTRACT**

Ion selective electrodes (ISEs) are analytical sensors that monitor the interactions between an ionophore within a polymeric membrane and ions in various solutions. The sensitivity and selectivity of ISEs is directly related to the chemical components. One type of ionophore utilized in ISEs are metalloporphyrins. Metalloporphyrins have unique binding characteristics, which make them useful in sensors. The polymeric membranes that are synthesized and used in ISEs consist of a metalloporphyrin complex, polyvinyl chloride, and *ortho*-nitrophenyl octyl ether. The membrane unique to this project contains erbium (III) tetraphenylporphyrin as the metalloporphyrin ionophore. Various analytical techniques were applied in the investigation of the reactivity and chemical characteristics of the metalloporphyrin complex within the membrane and in solutions. These techniques included gas chromatography, gas chromatography-mass spectrometry, ultraviolet-visible spectroscopy, and fluorescence spectroscopy. In this work, the optical properties of the erbium porphyrin complex, including major absorption and emission wavelengths, were examined. The applicability of several chromatographic techniques was also studied. The reactivity of the metalloporphyrin within the polymeric membrane was measured directly upon exposure to variable concentrations of the target analyte. In the future, the plan is to further investigate spectroscopic techniques such as fluorescence and the potential use of porphyrins in fluorescent indicators, much like the ISEs. The goal is to expand the knowledge of the porphyrin's reactivity to improve the sensitivity and selectivity of ion selective electrodes.

**KEYWORDS:** ion selective electrode, ionophore, metalloporphyrin, tetraphenylporphyrin, chromatography, spectroscopy

**INVESTIGATION OF THE INTERFACE REACTIONS OF ION SELECTIVE  
ELECTRODE MEMBRANES USING CHROMATOGRAPHIC AND  
SPECTROSCOPIC ANALYSES OF ERBIUM(III)  
TETRAPHENYLPORPHYRIN**

By

Alexis Rae Miller

A Master's Thesis  
Submitted to the Graduate College  
Of Missouri State University  
In Partial Fulfillment of the Requirements  
For the Degree of Master of Science, Chemistry

July 2021

Approved:

Erich D. Steinle, Ph.D., Thesis Committee Chair

Nikolay N. Gerasimchuk, Ph.D., Committee Member

Richard N. Biagioni, Ph.D., Committee Member

Michael J. Kyle, Ph.D., Committee Member

Julie Masterson, Ph.D., Dean of the Graduate College

In the interest of academic freedom and the principle of free speech, approval of this thesis indicates the format is acceptable and meets the academic criteria for the discipline as determined by the faculty that constitute the thesis committee. The content and views expressed in this thesis are those of the student-scholar and are not endorsed by Missouri State University, its Graduate College, or its employees.

## **ACKNOWLEDGEMENTS**

I would like to thank Dr. Erich Steinle for working as my advisor and mentor over the last few years. I would also like to thank the other members of my thesis committee including Dr. Nikolay Gerasimchuk, Dr. Richard Biagioni, and Dr. Michael Kyle for their time and energy helping me through my graduate studies. Lastly, I would like to thank the Department of Chemistry at Missouri State University for allowing me to participate in research both as an undergraduate and graduate student.

## TABLE OF CONTENTS

CHAPTER I. INTRODUCTION	1
1.1 Introduction to Metalloporphyrin-Based Polymer Membranes	1
1.2 Porphyrin Structures and Characteristics	2
1.3 Ion Selective Electrodes Background	6
1.4 Spectroscopy Theory and Methods	8
1.5 Chromatographic Methods	13
1.6 Goal of Research Project	15
CHAPTER II. EXPERIMENTAL METHODS	17
2.1 Materials	17
2.2 Gas Chromatography	17
2.3 Gas Chromatography Mass Spectrometry	19
2.4 UV-Visible Spectroscopy	21
2.5 Fluorescence Spectroscopy	28
CHAPTER III. RESULTS	30
3.1 Gas Chromatography Analysis	30
3.2 Gas Chromatography Mass Spectrometry Analysis	32
3.3 UV-Visible Spectroscopy Analysis of Porphyrin Solutions	34
3.4 UV-Visible Spectroscopy Analysis of Metalloporphyrin-Based Membranes	38
3.5 Fluorescence Spectroscopy Analysis	43
CHAPTER IV. DISCUSSION	45
4.1 Gas Chromatography	45
4.2 Gas Chromatography Mass Spectrometry	45
4.3 UV-Visible Spectroscopy of Porphyrin Solutions	46
4.4 UV-Visible Spectroscopy of Metalloporphyrin-Based Membranes	47
4.5 Fluorescence Spectroscopy	49
CHAPTER V. CONCLUSION AND FUTURE WORK	50
REFERENCES	52

## LIST OF FIGURES

Figure 1. Structure of a tetraazamacrocyclic porphyrin (left) and an N-confused isomer (right).	2
Figure 2. The two types of substituted porphyrins are (a) meso-substituted porphyrin and (b) $\beta$ -substituted porphyrin.	4
Figure 3. Structure of tetraphenylporphyrin, H <sub>2</sub> TPP.	4
Figure 4. Structure of erbium (III) tetraphenylporphyrin acetylacetonate.	5
Figure 5. Electronic state transitions that occur in the Soret and Q band regions.	12
Figure 6. UV-Visible spectrum of porphyrin complex with a zoomed in image of the Q bands.	13
Figure 7. Brightly colored porphyrin solution at different dates.	18
Figure 8. Freshly prepared porphyrin solution.	20
Figure 9. Erbium (III) tetraphenylporphyrin membrane solution with plasticizer and matrix.	23
Figure 10. Glass plate set-up (left) without the membrane solution, (middle) with the membrane solution, and (right) with the solidified membrane.	23
Figure 11. Small piece of membrane dissolved in THF.	24
Figure 12. Sliced glass microscopic slides approximately 8 mm for membrane films.	25
Figure 13. The three membrane films prepared and used for analysis using UV-Visible spectroscopy.	25
Figure 14. Initial chromatogram of the erbium (III) tetraphenylporphyrin solution in THF.	31
Figure 15. One-month old erbium (III) tetraphenylporphyrin solution in THF chromatogram.	32



Figure 16. GC-MS results of (top) erbium (III) tetraphenylporphyrin and (bottom) the identified compound <i>o</i> -nitrophenyl octyl ether.	33
Figure 17. (top) UV-Visible spectra of free tetraphenylporphyrin (H <sub>2</sub> TPP) and erbium (III) tetraphenylporphyrin in THF (bottom) spectra of the solutions from 450 to 700 nanometers.	36
Figure 18. (top) UV-Visible spectrum of erbium (III) tetraphenylporphyrin in THF and (bottom) Zoomed in spectrum of Q band region.	37
Figure 19. Membrane film A absorbance spectra in various aqueous solutions.	41
Figure 20. Membrane film B absorbance spectra in various aqueous solutions.	41
Figure 21. Membrane film C absorbance spectra in various aqueous solutions.	42
Figure 22. Membrane films A-C average absorbance spectra in various aqueous solutions.	42
Figure 23. Fluorescence spectrum at 420 nm excitation wavelength.	44
Figure 24. Fluorescence spectrum at 480 nm excitation wavelength.	44

## CHAPTER I. INTRODUCTION

### 1.1 Introduction to Metalloporphyrin-Based Polymer Membranes

Ion selective electrodes (ISEs) are analytical sensors that take advantage of a strong interaction between an ionophore that is placed within a plasticized polymeric membrane and analyte ions in the aqueous sample solution. The specific chemical components of the membranes used in ISEs are directly related to the sensitivity and selectivity of specific ions. Metalloporphyrins have been utilized as ionophores within ISEs and have been found to be selective for several analyte ions.<sup>1,2,3</sup> Metalloporphyrins have unique binding characteristics, which indicates their usefulness in sensors such as ISEs.<sup>4,5</sup> When the metalloporphyrin interacts with specific ions in the aqueous sample solution, it binds the ion and transports it into the non-polar polymer membrane. This transport process changes the balance of ions on either side of the ISE membrane, which produces a small but measurable phase boundary potential.<sup>4,6</sup> This voltage can be directly related to the analyte concentration via the well-known Nernst electrochemical equation.

Metalloporphyrins are one type of ionophores that can be used in ISEs.<sup>6,7</sup> They also have interesting optical properties that have also been utilized in biosensor applications.<sup>2,3,8</sup> The choice of metal that sits in the center of the porphyrin ring plays a major role in the selectivity of ions in a solution.<sup>9,10</sup> Many groups have examined metalloporphyrins with a wide variety of metals, which yields ISEs with selectivity for many different ions.<sup>1,4,9,10</sup> The identity of the metal produces a characteristic binding interaction with the ions in solution.<sup>2,8,11</sup>

## 1.2 Porphyrin Structures and Characteristics

The general porphyrin structure serves as the backbone and the binding site for the metal of choice when metalloporphyrins are formed. The core structure of a porphyrin is a tetraazamacrocyclic, which is an aromatic structure that connects four pyrrole molecules via bridging carbon atoms (Figure 1). The four nitrogen atoms from the pyrrole groups face each other in a relatively open cavity area. Porphyrins are known to be symmetric and are fairly rigid. The native form of the porphyrin is often abbreviated as  $H_2P$ , where  $H_2$  represents the two hydrogen atoms attached to two of the pyrrolic nitrogens and  $P$  is the porphyrin ring core. However, these two hydrogen atoms are easily deprotonated with the addition of a base, leading to the formation of a divalent anion porphyrin, abbreviated as  $P^{2-}$ . This dianion structure becomes a strong nucleophile that is capable of binding to cationic metals, which gives rise to the formation of many different metalloporphyrin compounds.

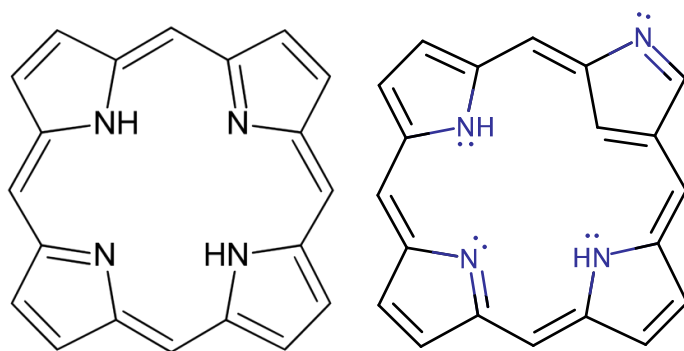


**Figure 1.** Structure of a tetraazamacrocyclic porphyrin (left) and an N-confused isomer (right).

Although the structure is typically rigid and unchangeable, there is an isomer that has been identified as a N-confused porphyrin (Figure 1). N-confused porphyrins are a pure isomer of tetrapyrrole macrocycle compounds where one of the pyrrole rings is flipped.<sup>12,13</sup> The flipping

of one of the pyrrole rings does not occur readily, which is explained by the intramolecular hydrogen bonds in the macrocyclic structure as well as by the aromaticity of the compound.<sup>12</sup> Although it does not readily occur, the confused porphyrin structure is known to be produced as a byproduct in some syntheses of porphyrin compounds. For example, in the synthesis of tetraphenylporphyrin, there is a small yield, approximately less than 5%, of the N-confused isomer.<sup>14</sup>

There are many other structural characteristics that can affect the reactivity of the porphyrin compounds. One important structural characteristic is the substituents that are connected to the outside of the core porphyrin macrocycle structure. Generally, the two types of substitution are meso- and  $\beta$ -substituted porphyrins (Figure 2). The choice of the outside species can significantly alter the nature of the entire porphyrin compound. For tetraphenylporphyrins, generally abbreviated as H<sub>2</sub>TPP (see Figure 3), four phenyl groups are attached to the four bridging carbons of the meso-porphyrin. Another common type of porphyrin is the octaethylporphyrin (H<sub>2</sub>OEP), where eight ethyl groups are attached to the carbon atoms within the pyrroles in the backbone of the  $\beta$ -porphyrin. The phenyl and ethyl groups in H<sub>2</sub>TPP and H<sub>2</sub>OEP, respectively, also impact the polarity of the overall molecule, making the resulting porphyrins more hydrophobic (or lipophilic), which is necessary for usage in ion-selective membrane electrodes.

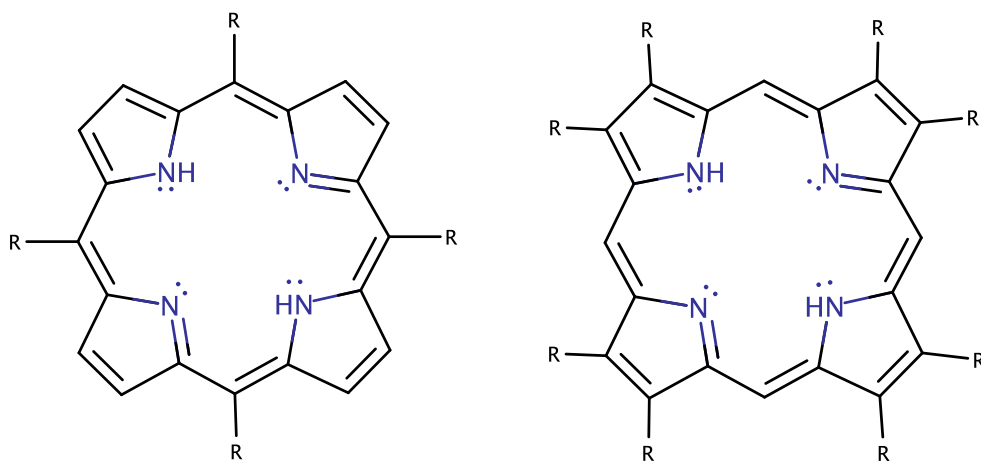


**Figure 2.** The two types of substituted porphyrins are (a) meso-substituted porphyrin and (b)  $\beta$ -substituted porphyrin.

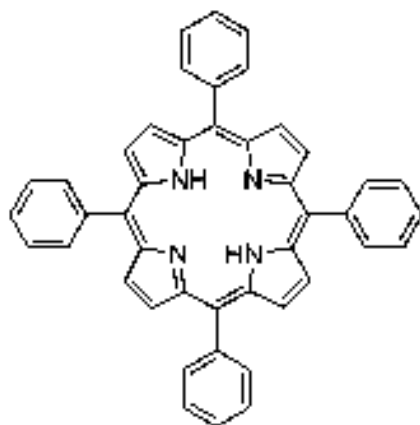


**Figure 3.** Structure of tetraphenylporphyrin, H<sub>2</sub>TPP.<sup>6,15</sup>

All metalloporphyrin compounds undergo two ring-centered reductions that give rise to metalloporphyrin  $\pi$ -anion radicals and dianions.<sup>15</sup> They also undergo two ring-centered oxidations that give rise to  $\pi$ -cation radicals and dications.<sup>15</sup> Non-planar metalloporphyrins have been known to be easier to oxidize than planar metalloporphyrins because of the distortion of the

macrocycle. In non-planar metalloporphyrins, the HOMO is destabilized, which creates a smaller HOMO-LUMO gap.<sup>15</sup> The magnitude of the HOMO shift is dependent on the specific metal ion and solution conditions.<sup>15</sup> Although the metal center can greatly affect the reactivity of the metalloporphyrin compound, there is still insufficient data regarding the effect of the oxidation state of the metal center. It is still unknown whether higher or lower oxidation states of the metal center are more stabilized or destabilized by non-planar metalloporphyrins.<sup>15</sup>

The polymeric membranes that are used in this research project utilize metalloporphyrins that contain the lanthanide metal erbium. Previous studies from members of the Steinle research group have demonstrated that erbium metalloporphyrin-based electrodes have selectivity for anions that contain carboxylic acid functionalities, such as salicylate and benzoate anions.<sup>16</sup> Erbium(III) tetraphenylporphyrin acetylacetonate, abbreviated as Er(III)TPP(acac), is a commercially available compound (see Chapter II: Experimental Methods), as seen in Figure 4.

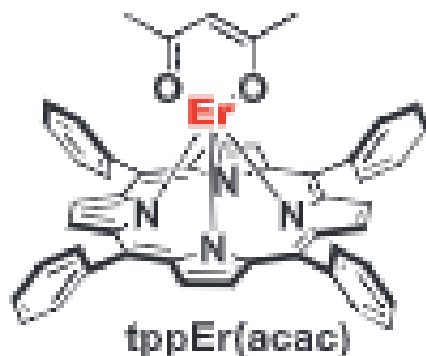


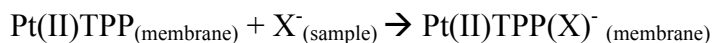
**Figure 4.** Structure of erbium (III) tetraphenylporphyrin acetylacetonate.<sup>17,18</sup>

### 1.3 Ion Selective Electrodes Background

Ion selective electrodes are sensors that have become widely used in analytical chemistry. Perhaps the most common example of an ISE is the common pH electrode. ISEs have grown to be a popular instrument for the analysis of solutions containing anions and cations. Although ISEs have become a common instruments, electrodes used to measure some specific ions are still being developed in laboratories across the world.<sup>11</sup> ISEs are used for many applications such as environmental analysis and physiology.<sup>5,6</sup> The key components of the electrodes are polymeric membranes and ion-binding lipophilic agents, known as an ionophore.<sup>5,19</sup> When an anion exchanger material such as tridodecylmethyl ammonium chloride (TDMAC) is utilized as the ionophore, the interaction between the ionophore and the target anions are based solely on electrostatic attraction. The selectivity of the resulting ISEs is known as the Hofmeister series ( $\text{ClO}_4^- > \text{SCN}^- > \text{salicylate}^- > \text{I}^- > \text{NO}_3^- > \text{Br}^- > \text{NO}_2^- > \text{Cl}^- > \text{HCO}_3^- > \text{F}^-$ ), which is based solely on the hydrophobicity of the anions.<sup>11,20,21</sup> Anions such as perchlorate ( $\text{ClO}_4^-$ ) and thiocyanate ( $\text{SCN}^-$ ) can be measured easily with these anion-exchanger ISEs, but anions at the bottom of the series, such as chloride and fluoride, are much more difficult to measure. When an ionophore that has specific binding towards a particular analyte ion is utilized, the resulting selectivity patterns deviate significantly from the Hofmeister series. Metalloporphyrin-based ISEs have demonstrated very interesting selectivity patterns that are specific to the choice of metal incorporated into the porphyrin ionophore. For example, indium(III) and gallium(III) octaethylporphyrin-based ISEs have selectivity towards the anions chloride and fluoride, respectively.<sup>11</sup>

Metalloporphyrin-based ISEs have two well-established response mechanisms. The first is called the neutral carrier mechanism, where a divalent metal cation such as platinum(II) sits

within the doubly deprotonated porphyrin core. The resulting metalloporphyrin is neutral (for example Pt(II)TPP or Zn(II)OEP) and binds with target anions at the membrane/sample interface via a neutral carrier mechanism.

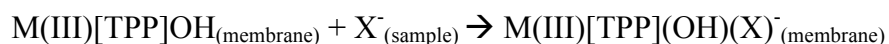


However, when a trivalent metal is utilized, the resulting metalloporphyrin is also positively charged. For example, when gallium(III) is utilized, positively charged Ga(III)[OEP]<sup>+</sup> is formed. When these metalloporphyrins are utilized, a charged carrier mechanism is prevalent.

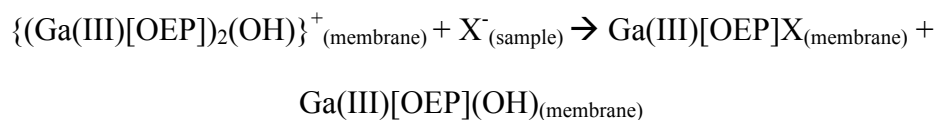


The metals within the porphyrin ring assume an octahedral configuration, with all four of the equatorial binding positions taken by the nitrogen atoms within the porphyrin. This leaves two axial positions, above and below the plane of the metalloporphyrin, free to bind the target anion.

However, the possibility of a trivalent metalloporphyrin assuming a neutral carrier mechanism is possible. In this case, the metal has a permanent fifth axial ligand anion, but still could bind to an analyte anion in the remaining sixth axial position.



ISEs based on metalloporphyrins with trivalent (or higher) metals have at least two different response mechanisms possible. Steinle, et al., discovered that some metalloporphyrins can assume a dimeric or aggregated configuration within the membrane, leading to a unique charged carrier mechanism where the dimer is broken into monomers upon exposure to the target anion.<sup>9</sup>





After finding the correct response mechanism, the membrane composition can be optimized to achieve the best possible selectivity patterns. Generally, this is achieved via the addition of lipophilic ionic additives (positively charged additives for neutral carrier mechanisms and negatively charged additives for charged carrier mechanisms).<sup>22</sup>

To date, the Steinle research group at Missouri State University has focused primarily on ISEs based on metalloporphyrins lanthanide metals such as lutetium and erbium.<sup>22</sup> As mentioned previously, the Er(III)TPP(acac)-based ISEs have demonstrated non-Hofmeister selectivity patterns with a preference towards anions that contain carboxylate acid groups. However, the nature of the response mechanism of interaction between Er(III)TPP(acac) and the analyte anions has not been examined in detail. For this project, analytical methods other than traditional electroanalytical potentiometry such as spectroscopy and chromatography were utilized. The primary goal of this project was to better understand the response mechanism of the Er(III)TPP(acac)-based ISEs, with the ultimate goal of improving the response characteristics of the ISEs towards the target anions.

#### **1.4 Spectroscopy Theory and Methods**

Spectrometric methods of analysis consist of many analytical techniques based on atomic and molecular spectroscopy. Spectroscopy is defined as the interactions of radiation with matter.<sup>23</sup> Many instruments that perform spectroscopic analyses are considered to be optical instruments. Optical instruments can measure various regions including the ultraviolet (UV), visible, and infrared (IR) regions parts of the electromagnetic spectrum. Optical spectroscopic methods are based on six phenomena: adsorption, fluorescence, phosphorescence, scattering, emission, and chemiluminescence.<sup>23</sup>

Typical spectroscopic instruments are made up of five major components: a source of radiant energy, a wavelength selector, a container that holds the sample, a radiation detector which converts the radiation into an electrical signal, and a signal processor / readout device.<sup>23</sup> Both absorption and fluorescence require an external source of radiation.<sup>23</sup> In absorption, the source beam passes through a wavelength selector then through the sample.<sup>23</sup> In fluorescence, the source induces the sample to emit unique radiation that is then measured at a 90° angle from the source.<sup>23</sup>

There are many types of optical instruments that can be used in spectroscopic investigations. With a spectrophotometer, the user can vary the wavelength of the source light via a wavelength selector such as a monochromator. A spectrofluorometer is a spectrophotometer used for fluorescence measurements, which utilizes two monochromators, one for light from the source and another for the fluorescent light emitted from the sample. Some advantages of spectrophotometric and photometric methods of analysis include a wide range of applicability, low detection limits of  $10^{-4}$ - $10^{-5}$  M, high selectivity, and good accuracy.<sup>23</sup>

**Ultraviolet-Visible Spectroscopy.** Molecular absorption spectroscopy is used in the quantitative analysis of many inorganic, organic, and biological compounds.<sup>23</sup> It can measure absorption in both the ultraviolet (UV) and visible regions. UV-visible spectroscopy can also be used in the identification of molecules in fields such as environmental chemistry, forensic science, and clinical laboratories.<sup>23</sup> Measurements are based on the transmittance or absorbance of solutions in cells with a standard path length.<sup>23</sup>

A UV-visible spectroscopy instrument is made up of a source, wavelength selector, sample container, radiation transducer, and a signal process and readout device. Light that is not absorbed by components in the sample container makes its way to the detector. The ratio of light

from the source ( $P_0$ ) and the light that passes through the sample ( $P$ ) is used in Beer's Law to calculate absorbance ( $A$ ), which is directly correlated to analyte concentration ( $c$ ).

$$A = -\log T = \log \frac{P_0}{P} = \epsilon bc$$

UV-visible spectroscopy can also be useful in monitoring the equilibrium between monomer and dimer conformations of complex structures.<sup>24</sup> Absorption of radiation in the UV-visible regions occurs in one or more electronic bands.<sup>23</sup> These bands are made up of many discrete lines that arise from the transition of an electron from the ground state to an excited vibrational or rotational electronic energy state.<sup>23</sup>

**Fluorescence Spectroscopy.** Fluorescence is a phenomenon produced when electrons within molecules in a solution are excited and upon relaxation back to the ground state emit radiation that can provide unique information for qualitative and quantitative analyses.<sup>23</sup> The intensity of this photoluminescence allows for the quantitative measurement of various compounds in trace amounts. There are many advantages to luminescence methods of analysis including the sensitivity and detection limits that are generally three orders of magnitude lower than absorption spectroscopy.<sup>23</sup> These methods also have large linear concentration ranges that are significantly greater than absorption spectroscopy.<sup>23</sup> Although there are some advantages to using luminescence methods over absorption methods, there are also a few disadvantages. Luminescence techniques are not as applicable as absorption methods because more compounds absorb ultraviolet and visible radiation than exhibit photoluminescence in the same regions.<sup>23</sup>

The excitation in fluorescence is due to the absorption of energy from incoming photons.<sup>23</sup> Fluorescence occurs in both simple and complex gaseous, liquid, and solid compounds.<sup>23</sup> The molecular structure determines the native ability to fluoresce and intensity of emission, which is why this method of analysis can be used to identify unique chemical

characteristics. The excited states are short lived ( $<10^{-5}$  s) because there is not a change in electron spin in the electronic energy transitions.<sup>23</sup> Fluorescence occurs when a photon is excited and transitions from the lower vibrational level of the first excited state to a vibrational level in the ground state.<sup>23</sup> Fluorescence is the most intense in aromatic compounds that allow for  $\pi \rightarrow \pi^*$  transitions that are lower in energy.<sup>8,23,25</sup> Rigid structures also are known to prefer fluorescent emissions.

The emission intensity of fluorescence is measured as a function of wavelength at a fixed excitation wavelength. The instrument is made up of many components similar to those discussed previously for absorption instruments. The source radiation passes through the excitation wavelength selector, then impacts the sample, which excites the sample causing it to emit fluorescent photons.<sup>23</sup> The emitted radiation is then isolated by the emission wavelength selector.<sup>23</sup> After passing through the emission wavelength selector, the remaining photons pass through a phototransducer that converts the radiation into electrical signal.<sup>23</sup> There are multiple types of instruments that can be used to measure the fluorescence of chemical systems. For example, a fluorometer is an instrument containing the typical components, but it only uses filters for wavelength selectors.<sup>23</sup> A spectrofluorometer also uses two monochromators for wavelength selectors.<sup>23</sup> The unique selectivity of spectrofluorometers are beneficial in the electronic and structural characterizations of various molecules and are widely used in analytical analyses.<sup>23</sup>

**Porphyrin Spectroscopy.** The porphyrin complexes are known to have intense colors due to their highly conjugated  $\pi$ -systems.<sup>1,25</sup> The vibrant colors also illustrate their distinctive spectra in the ultraviolet-visible region.<sup>1</sup> Both the porphyrin complex and the metal center produce peaks in the ultraviolet visible region. These two sets of bands produced are Soret and Q

bands. Soret bands depend on the substitution of porphyrin complex and usually result in peaks between 380-500 nm.<sup>1,17,26,27,28</sup> The transition that is normally observed is from the singlet ground state to the second singlet excited state (Figure 5).<sup>1</sup> The Q bands result from the transition from the singlet ground state to the first excited state and produce four peaks between 500-750 nm, which is due to the vibrational splitting (Figure 5).<sup>1,17,26,27,28</sup> The red shift is due to the effects of ring substitution as well as the conformation of the macrocyclic porphyrin in the solution.<sup>29</sup> The metal centers also contribute to the presence of the Q bands. The stability of the metal determines the intensities of the peaks.<sup>1</sup> A typical UV-visible spectrum of an etio-type porphyrin can be found below (Figure 6).<sup>1</sup> The type of porphyrin is based on the intensities of the four Q-bands. This particular example of a porphyrin is  $\alpha$ -substituted with alkyl groups.<sup>1</sup> Using the knowledge provided by previous research using UV-visible spectroscopy, the analysis of the erbium porphyrin complex can be performed to compare the porphyrin characteristics.

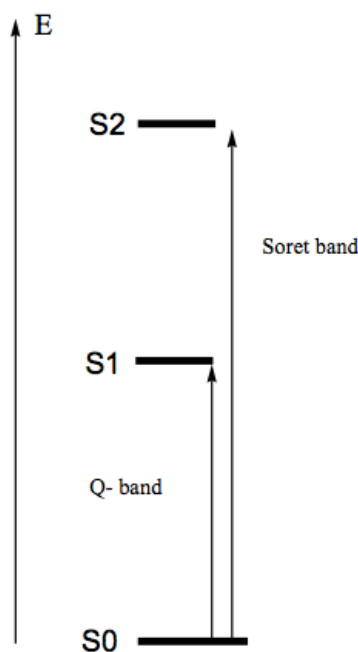


**Figure 5.** Electronic state transitions that occur in the Soret and Q band regions.

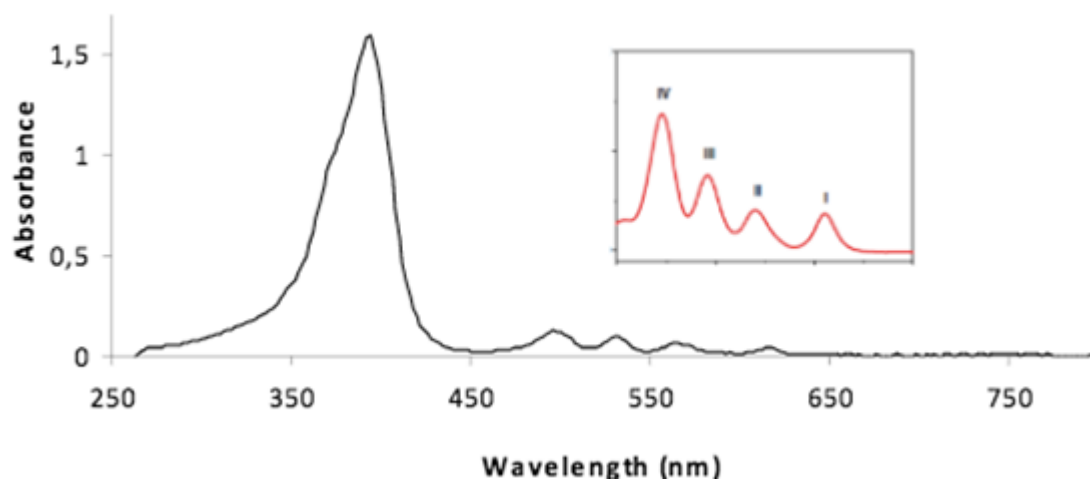


**Figure 6.** UV-Visible spectrum of an etioporphyrin complex with a zoomed in image of the Q bands.<sup>1</sup>

### 1.5 Chromatographic Methods

The analysis of individual compounds in a mixture can be difficult, so separation techniques can be beneficial in removing potential interferences from the desired analyte. One of the most common separation techniques is chromatography.<sup>23</sup> Chromatography is defined as a form of separation that can lead to the identification of similar chemical components of complex mixtures, which can be difficult to achieve using other analytical techniques.<sup>23</sup> Chromatographic methods of analysis have become a widely popular analytical technique with various applications. In chromatographic methods, a mobile phase is used to transport a sample.<sup>23</sup> The mobile phase can be a gas, liquid, or a supercritical fluid.<sup>23</sup> The mobile phase is then sent through a stationary phase that is fixed in either a column or on a solid surface.<sup>23</sup> The components of the sample move in and out of the mobile and stationary phases depending on their relative interactions, causing unique distribution of migration rates of the chemical components.<sup>23</sup> For example, a molecule that spends more time in the stationary phase will elute off the column later

than a molecule that does not have as much interaction with the stationary phase. The differing migration rates allow for the components of the sample to elute into discrete bands that can qualitatively and quantitatively be used to describe the chemical system.<sup>23</sup>

Chromatography can be classified based on the type of mobile and stationary phase. The three categories are gas chromatography (GC), liquid chromatography (LC), and supercritical fluid chromatography.<sup>23</sup> The mobile phases in these respective techniques are gas, liquid, and supercritical fluids. Liquid chromatography is the only method that can use either packed columns or planar surfaces for the interaction between the stationary phase and mobile phase.<sup>23</sup> The column used in methods such as gas chromatography is made of a narrow tube coated on the inside wall with the stationary phase.<sup>23</sup> As the sample solution and mobile phase pass through the column, the chemical components interact with the stationary phase and produce a unique separation as they elute off the column. The detector then identifies the concentration of each chemical versus time to create a chromatogram that can be used to identify the components of a solution.<sup>23</sup> The retention times are a defining characteristic of molecular identity and the size of the chromatographic peaks can be used to determine the amount of each component present.<sup>23</sup> The qualitative information provided by the retention times allows for the identification of the chemical components present as well as the compounds that are not present or undetectable.

The main components of a gas chromatography instrument include a carrier gas system, flow regulators, sample injector system, column, oven, and detector with a data output reader.<sup>23</sup> Generally, the variable components of a GC instrument include the injection temperature, stationary phase composition, oven temperature, and type of detector. Each component is chosen specifically based on the type of molecules in the sample to be measured.

Recently, gas chromatography instruments with mass spectrometry detectors (abbreviated as GC-MS) have become popular in the recent decades due to the information that is provided by the detector. Instrumentation for a GC-MS includes all the components previously mentioned along with a mass spectrometer added as a detector. The combination of gas chromatography with mass spectrometry has greatly increased the instrument's applicability and usefulness in the identification of components of a sample. An ionization source takes molecules that elute from the column and converts them to ions. The mass spectrometer measures the mass-to-charge ratios of the produced ions correlated to the time for which the component of the sample passes through the MS detector. With this data, a mass fragmentation pattern is produced which is representative of the molecular component. Libraries of mass fragmentation patterns of known compounds can be used to identify the components of a sample.<sup>23</sup> Gas chromatography-mass spectrometry has become the most widely used technique for separating and identifying chemical components in a solution.<sup>23</sup> The National Institute for Standards and Technology (NIST) formed a mass spectral data base consisting of 250,000 compounds with 70,000 retention indices.<sup>23</sup> The software application NIST also created has the ability to match experimental data to those of known compounds for more accurate identification.<sup>23</sup>

## **1.6 Goal of Research Project**

The purpose of this research project was to better understand the reactivity of the porphyrin membrane utilized in the ion selective electrodes by analyzing the ionophore Er(III)TPP(acac). Membranes and solutions containing this molecule were analyzed using different analytical techniques to help understand the reactions that occur on the interface of the membrane with specific anions in the sample solution. Specifically, chromatographic techniques



can describe the unique retention times of the complex and mass spectrometry can calculate the mass to charge ratio. Spectroscopic techniques describe the optical properties including the absorption wavelengths of the complex as well as reveal the possibility of dimerization of the Er(III)TPP(acac) within the membrane. Understanding these reactions can lead to a greater selectivity and sensitivity of the resulting ion selective electrodes.

## CHAPTER II. EXPERIMENTAL METHODS

### 2.1 Materials

Erbium(III) meso-tetraphenylporphine 2,4-pentane dionate was obtained from Frontier Scientific (Newark, Delaware) and used as received. Tetraphenylporphyrin was obtained from Mid-Century (Chicago, Illinois) and used as received. Erbium(III) acetate hydrate, 2-nitrophenyl octyl ether, poly(vinyl chloride), sodium benzoate, 2-(N-morpholino)ethane sulfonic acid (MES) hydrate, MES sodium salt and tetrahydrofuran were obtained from Sigma Aldrich (St. Louis, Missouri) and used as received.

### 2.2 Gas Chromatography

**Sample Preparation.** The procedure consisted of the preparation of the erbium(III) tetraphenylporphyrin solution and the analysis of the sample using different techniques. First, the metallic porphyrin in a tetrahydrofuran (THF) solvent was prepared. A fairly low concentration was prepared to ensure the sample would be appropriate for gas chromatography. Other samples were prepared including tetraphenylporphyrin in THF and erbium(III) acetate hydrate in THF to understand the different aspects of the compound.

Erbium(III) Tetraphenylporphyrin Solution. Approximately 2.1 mg of erbium(III) meso-tetraphenylporphyrin was measured into a small glass vial. 20.0 mL of THF solvent was added to the vial. Then the vial was vortexed to ensure a homogeneous mixture. The concentration of the metallic porphyrin solution was  $1.2 \times 10^{-4}$  M (Figure 7).

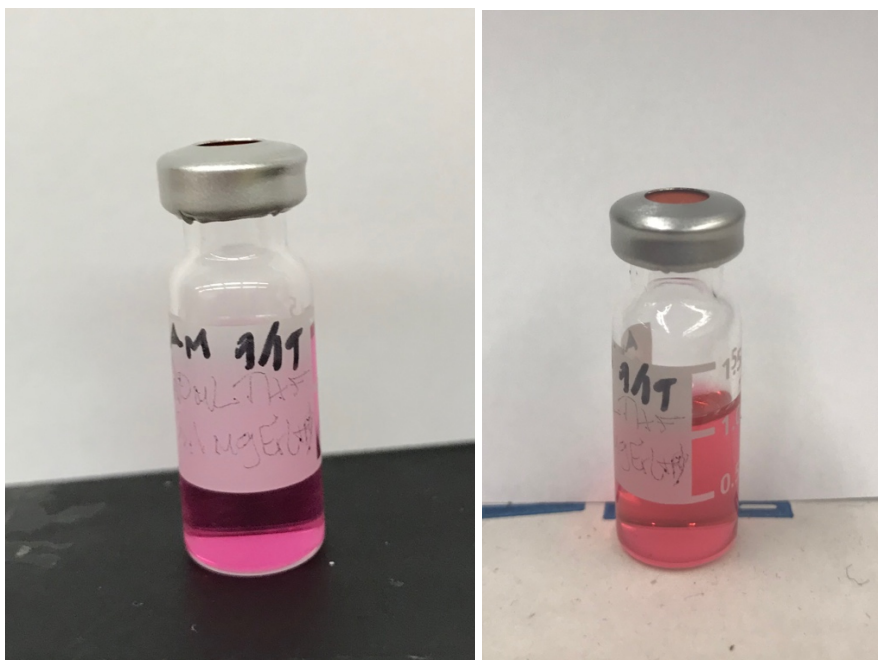


**Figure 7.** Brightly colored porphyrin solution at different dates. The first image is of a freshly made solution and the second image is the same solution a month later.

Tetraphenylporphyrin Chlorine Free Solution. The non-metalated porphyrin solution was prepared by measuring 1.8 mg of tetraphenylporphyrin into a small glass vial. Using a pipette, 20.0 mL of THF was transferred to the vial containing the tetraphenylporphyrin compound. Then the solution was vortexed to ensure a homogeneous mixture. The concentration of the tetraphenylporphyrin solution was  $1.3 \times 10^{-4}$  M.

Erbium(III) Acetate Hydrate Solution. The erbium solution was prepared by measuring 1.8 mg of erbium(III) acetate hydrate into a small glass vial. Using a pipette, 20.0 mL of THF was transferred to the vial containing the erbium compound. Then the solution was vortexed to ensure a homogeneous mixture. The concentration of the erbium(III) acetate hydrate solution was  $2.6 \times 10^{-4}$  M.

**Instrumentation and Reaction Conditions.** The first technique used to analyze the sample solutions was gas chromatography. The instrument used was Varian 430 G.C. with a

Restek 30 m length and 0.53 mm diameter column with a maximum temperature of 290°C. Other instrument parameters included an injector temperature of 300°C, detector temperature of 300°C, oven temperature of 200°C, and an injector flow of 112.1 mL/min. The parameters included in the method was an initial temperature of 200°C for 2.00 minutes, ramp of 20°C/min, and final temperature of 290°C (held for 10.0 minutes). Changes were made to the method throughout experiments to analyze the effects on the chromatogram.

**Procedure.** Once all of the different solutions were prepared, a small portion of each was added to autosampler vials and placed in the autosampler. The first solution that was measured was the Er(TPP)acac in THF solution. Then the H<sub>2</sub>TPP and the erbium metal solutions were measured. Lastly, the pure THF solution was measured. Each solution was analyzed multiple times to ensure the chromatograms were reproducible.

## 2.3 Gas Chromatography Mass Spectrometry

**Sample Preparation.** The second technique used was gas chromatography mass spectrometry. A fresh sample was prepared using the same erbium(III) tetraphenylporphyrin compound and the solvent THF. Approximately 1.4 mg of erbium(III) tetraphenylporphyrin was measured into a small glass vial. Using a pipette, 20.0 mL of THF was transferred to the vial containing the porphyrin compound. Then the solution was vortexed to ensure a homogeneous mixture. The concentration of the porphyrin solution was  $8.0 \times 10^{-5}$  M (Figure 8).



**Figure 8.** Freshly prepared porphyrin solution.

**Instrumentation and Reaction Conditions.** The instrument used was Agilent Technologies 7820A GC System. The column that was used was an HP-5 with a length of 30 m, diameter of 0.250 mm, and 0.25  $\mu\text{m}$  film. The maximum temperature of the column was 325°C and thermal auxiliary temperature of 275°C. The method that was used for all measurements included a 50.0 g- 1000 g mass range, 3 minute solvent delay, injector temperature of 300°C, 1  $\mu\text{L}$  injection volume, PFTBA calibration compound, and an ether and hexane washing between injections.

**Procedure.** Once the sample was prepared, a small portion of the solution was added to a vial and placed in the autosampler. The sample that was measured was  $8.0 \times 10^{-5}$  M Er(TPP) in THF. The run started with a 4-minute solvent delay but was later altered to a 3-minute solvent delay and a 2-minute delay. All other parameters remained constant during the many trial runs.

## 2.4 UV-Visible Spectroscopy

**Sample Preparation.** The third technique used was UV-visible spectroscopy. The previously prepared solutions used for gas chromatography as well as a freshly made solution were used for these measurements. A second sample was made a week later by measuring 1.9 mg of erbium(III) tetraphenylporphyrin into another small glass vial. Using a pipette, 20.0 mL of THF was transferred to the vial containing the erbium compound. Then the solution was vortexed to ensure a homogeneous mixture. The concentration of the second solution was  $1.1 \times 10^{-4}$  M.

**Porphyrin Solution Instrumentation and Reaction Conditions.** The instrument used was Agilent Cary 60 UV-vis spectrophotometer. The parameters included a wavelength range of 200-800 nm, 0.2 second average time, 1.0 nm intervals, 300 nm/min, and 2.0-minute scan time. A quartz cuvette containing THF was measured to form a baseline that was used for all following measurements.

A second instrument was used in the UV-visible spectroscopy technique for more precise results of the analysis of the porphyrin complex. The instrument was UV-Vis Lambda 650 Perkin Elmer. The parameters included data intervals of 0.5 nm and data range of 250- 800 nm. The instrument was also calibrated using an empty quartz cuvette.

**Porphyrin Solution Procedure.** Using the first UV-visible spectrophotometer, the  $1.1 \times 10^{-4}$  M Er(TPP) in THF solution was measured. Following the porphyrin solution, the H<sub>2</sub>TPP and erbium metal solutions were also measured and compared to the spectrum of the porphyrin solution. Each solution was transferred to a clear quartz cell for analysis using a glass pipette. Using the second UV-Vis Lambda Perkin Elmer instrument, a freshly made porphyrin solution with  $1.08 \times 10^{-4}$  M concentration was measured. The solution was transferred to a clear quartz

cell for analysis using a glass pipette. The instrumental parameters remained consistent for each sample.

**Porphyrin Membrane Film Preparation.** The last aspect was the determination of the optical properties of the erbium(III) tetraphenylporphyrin complex in the membrane. The experimental methods were adopted from Dr. Steinle's graduate work with metalloporphyrin-based liquid/polymer membrane electrodes.<sup>9</sup>

Erbium(III) Tetraphenylporphyrin Membrane. The first step in preparation was the synthesis of a fresh membrane composed of the metalloporphyrin compound, polyvinyl chloride (PVC), and 2-nitrophenyl octyl ether (*o*-NPOE). Approximately 2.0 mg of erbium(III) tetraphenylporphyrin was measured along with 123.8 mg of *o*-NPOE and 60.5 mg of PVC (Figure 9). This unique composition is the method of preparation used for many preparations of porphyrin membranes with about 1% metalloporphyrin, 66% plasticizer, and 33% matrix. For the formation of the membrane, a flat glass plate was used along with a glass ring, which was held in place using rubber bands (Figure 10). Once all three components were homogeneous using the vortex, the solution was transferred using a glass pipette to the glass ring on the glass plate (Figure 10). The entire set-up was left for 24 hours to allow for the membrane to form (Figure 10).



**Figure 9.** Erbium (III) tetraphenylporphyrin membrane solution with plasticizer and matrix.

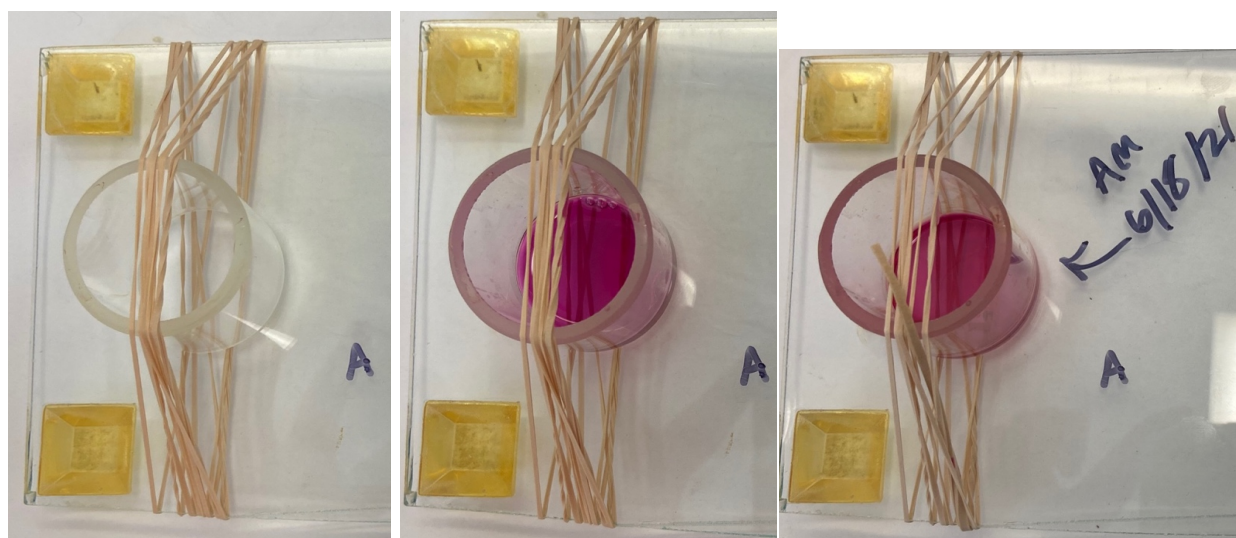


**Figure 10.** Glass plate set-up (left) without the membrane solution, (middle) with the membrane solution, and (right) with the solidified membrane.

Erbium(III) Tetraphenylporphyrin Membrane Film. Using the freshly made membrane, the thin films were prepared. First, a small piece of the membrane, approximately 5 mg and 5-6 mm in diameter, was cut out and placed in a glass vial. Then the membrane was dissolved in as



little THF as possible. Small amounts of THF were slowly added using a glass pipette and vortexed until the membrane completely dissolved, and the solution became homogeneous (Figure 11). The amount of THF required for each thin film preparation varied, but was around 1-2 mL. For further analysis, glass slides were created for the films. A thin piece, approximately 8 mm, was sliced from a microscopic slide using a glass cutter to create a slide that fit inside a plastic cuvette (Figure 12). Multiple slides were cut for potential use for the thin film analyses (Figure 12). The membrane solution was then slowly pipetted onto the glass slide, which was placed on a level glass plate. Slowly adding the solution onto the glass slide allowed for the solution to settle on the glass slide without spilling over the sides, which would have affected the concentration of the porphyrin in the film. After the entire solution, approximately 1-2 mL, was transferred to the glass slide, the slide remained on the glass plate to allow for the THF to evaporate off and the film to dry (Figure 13). Once the film was dry, it was placed in a plastic cuvette for analysis using UV-visible spectroscopy. Three different membrane films were prepared and analyzed (Figure 13).



**Figure 11.** Small piece of membrane dissolved in THF.

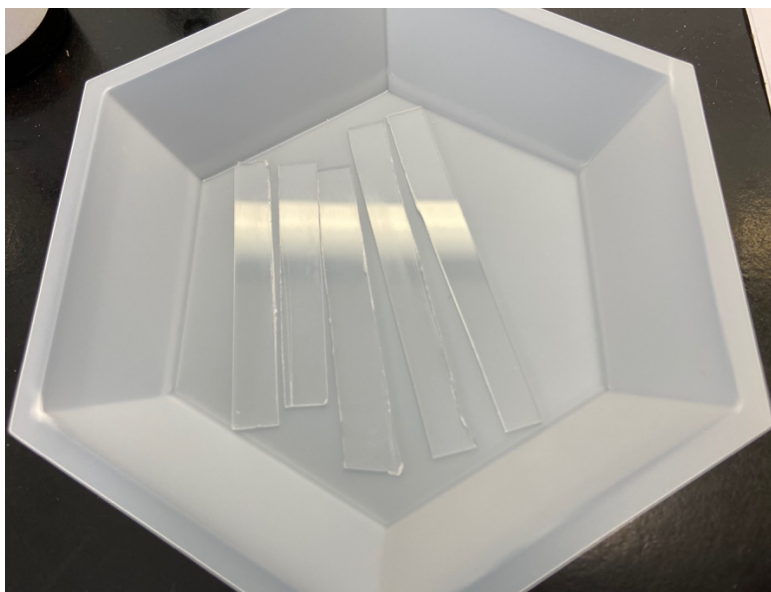


**Figure 12.** Sliced glass microscopic slides approximately 8 mm for membrane films.

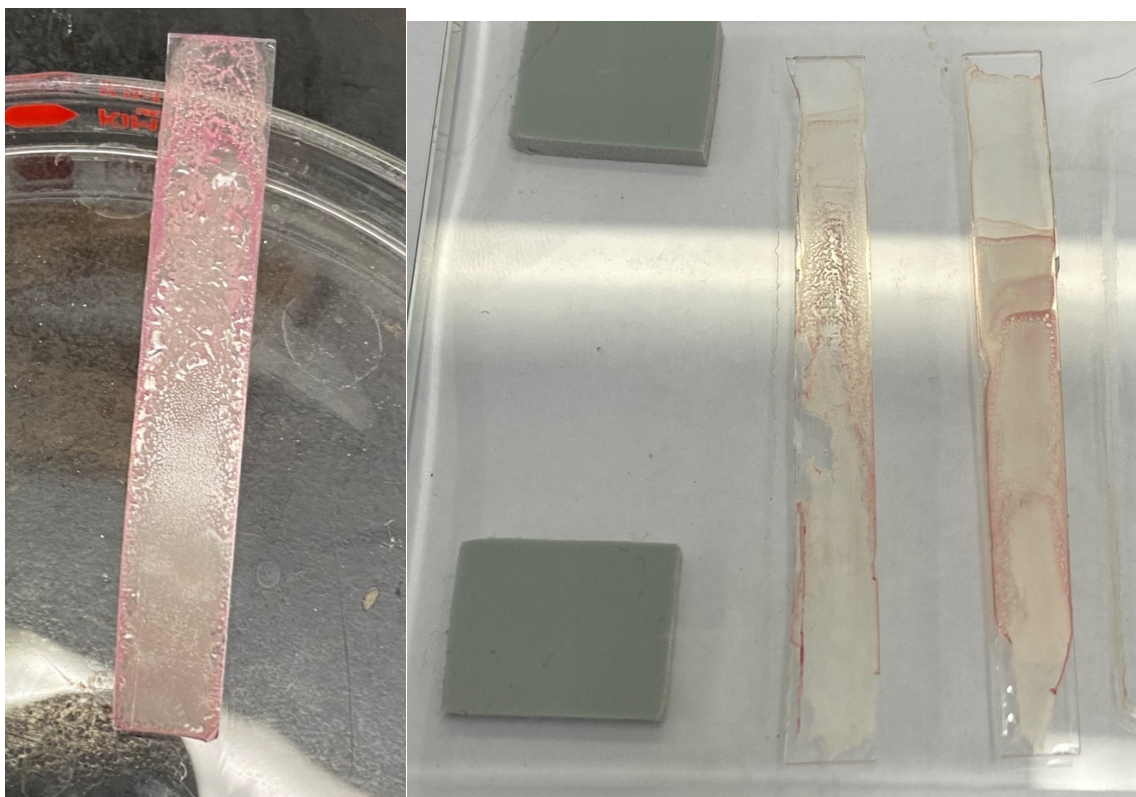


**Figure 13.** The three membrane films prepared and used for analysis using UV-Visible spectroscopy.

Morpholino Ethanesulfonic Acid (MES) Buffer Solutions. The thin membrane films were analyzed in various MES buffer solutions that were prepared. A stock MES buffer solution of 0.05 M was prepared with approximately 7.8251 g of MES hydrate and 1.9519 g of MES sodium salt, which was transferred to a volumetric flask and diluted to 1.0 L using DDI water. The solution was mixed until it was homogeneous. A set of various buffer solutions containing sodium benzoate were also prepared. The concentrations ranged from  $1 \times 10^{-5}$  M to  $1 \times 10^{-2}$  M sodium benzoate. Each solution was prepared by diluting 0.01 M, 0.1 M, and 1 M sodium benzoate solutions used for other electrode experiments. The first solution was made by measuring out 100  $\mu$ L of 0.01 M sodium benzoate using a micropipette, which was transferred to a 100 mL volumetric flask and diluted using the stock 0.05 M MES buffer solution previously prepared. The concentration of the buffer solution was  $1 \times 10^{-5}$  M sodium benzoate in MES. Once the solution was made, it was transferred to a labeled glass bottle for easier transfers to the cuvettes. The next solution was made by measuring 1,000  $\mu$ L of 0.01 M sodium benzoate using a micropipette, which was transferred to a 100 mL volumetric flask and diluted using the stock 0.05 M MES buffer solution. The concentration of the buffer solution was  $1 \times 10^{-4}$  M sodium benzoate in MES. Once the solution was made, it was transferred to a labeled glass bottle. The next solution was made by measuring 1,000  $\mu$ L of 0.1 M sodium benzoate using a micropipette, which was transferred to a 100 mL volumetric flask and diluted using the stock 0.05 M MES buffer solution. The concentration of the buffer solution was  $1 \times 10^{-3}$  M sodium benzoate in MES. Once the solution was made, it was transferred to a labeled glass bottle. The next solution was made by measuring 1,000  $\mu$ L of 1 M sodium benzoate using a micropipette, which was transferred to a 100 mL volumetric flask and diluted using the stock 0.05 M MES buffer

solution. The concentration of the buffer solution was  $1 \times 10^{-2}$  M sodium benzoate in MES. Once the solution was made, it was transferred to a labeled glass bottle.

**Porphyrin Membrane Film Instrumentation and Reaction Conditions.** The instrument used was Agilent Cary 60 UV-vis spectrophotometer. The parameters included were a wavelength range of 370-500 nm, 0.15 nm data interval, and 0.100 s average scan time. The baseline was set as the measurement of an empty plastic cuvette. The first run was performed on the dry membrane without any buffer solution. The buffer solutions were then placed in multiple plastic cuvettes. The cuvettes were then placed in the instrument to measure the absorbance of the membrane film in each solution. The three membrane films prepared were measured in the various buffer solutions to provide triplicate results to indicate the potential for repetition. Each measurement was performed in duplicate to ensure precision.

**Porphyrin Membrane Film Procedure.** The first porphyrin membrane (A) was prepared on the glass microscopic slide and placed in an empty plastic cuvette for analysis of the dry membrane. The first run was performed on the dry membrane to analyze the changes that occur to the membrane in various buffer solutions. The next run was performed on the membrane film in the stock 0.05 M MES buffer solution. For the measurements of the membrane films in the buffer solutions, the film was placed in the cuvette containing the buffer solution and allowed for equilibrium to be reached before the absorbance was measured. The films were placed in the buffer solutions for approximately 10 minutes, which is the time it takes to reach equilibrium in the electrode experiments. After the first membrane film (A) sat in the 0.05 M MES buffer solution, the absorbance was measured using the parameters previously described. The solution was measured twice to ensure precision between each run. Then the membrane film (A) was removed from the cuvette and placed in a cuvette containing the  $1 \times 10^{-5}$  M sodium benzoate in

MES buffer solution. It was again equilibrated for approximately 10 minutes prior to the runs. Once the solution had equilibrated, the absorbance was measured twice. The same procedure was performed for the remaining solutions including the  $1 \times 10^{-4}$  M,  $1 \times 10^{-3}$  M, and  $1 \times 10^{-2}$  M sodium benzoate in MES buffer solutions. The first membrane film (A) was placed in all of the different buffer solutions and the changes and absorbance were measured. Once the first membrane film (A) was measured in all of the solutions, the second membrane film (B) was prepared. The same procedure was performed on the second membrane film (B) with the order of runs as follows: dry membrane (x2), 0.05 M MES (x2),  $1 \times 10^{-5}$  M sodium benzoate in MES (x2),  $1 \times 10^{-4}$  M sodium benzoate in MES (x2),  $1 \times 10^{-3}$  M sodium benzoate in MES (x2), and  $1 \times 10^{-2}$  M sodium benzoate in MES (x2). Once the second membrane film (B) was measured in all of the solutions, the third membrane film (C) was prepared. The same procedure was performed on the third membrane film (C) with the order of runs as follows: dry membrane (x2), 0.05 M MES (x2),  $1 \times 10^{-5}$  M sodium benzoate in MES (x2),  $1 \times 10^{-4}$  M sodium benzoate in MES (x2),  $1 \times 10^{-3}$  M sodium benzoate in MES (x2), and  $1 \times 10^{-2}$  M sodium benzoate in MES (x2).

## 2.5 Fluorescence Spectroscopy

**Sample Preparation.** The last optical technique used was fluorescence spectroscopy. The porphyrin solution prepared for gas chromatography mass spectrometry was used for these measurements.

**Instrumentation and Reaction Conditions.** The instrument used for fluorescence spectroscopy was the Perkin Elmer LS55 Fluorescence Spectrometer. The parameters that were used included an emission wavelength range of 380 nm-900 nm and a scan speed of 100 nm/minute. The excitation wavelength and excitation and emission slit widths were altered

between runs. The initial excitation wavelength was 420 nm. The other excitation wavelength that was measured was 480 nm. The initial excitation and emission slit widths were both 2.5 nm, but was later adjusted to 10.0 nm for clearer spectrums.

**Procedure.** The previously prepared solution ( $8.0 \times 10^{-5}$  M Er(TPP) in THF) was transferred to a quartz cuvette using a glass pipette. Then the cuvette was placed in the instrument and the parameters were selected. The first run consisted of an excitation wavelength of 420 nm and excitation and emission slit widths of 2.5 nm. Since the first run was very noisy, the excitation and emission slit widths were adjusted to 10.0 nm for another run. Then the excitation wavelength was changed to 480 nm and the major peaks of emission were noted.

## CHAPTER III. RESULTS

### 3.1 Gas Chromatography Analysis

Modern ion-selective electrodes generally consist of an ionophore, plasticizer and polymeric material. In the previous studies by the Steinle group, erbium(III) tetraphenylporphyrin, ortho-nitrophenyl ethyl ether (*o*-NPOE) and polyvinyl chloride (PVC) were utilized as the ionophore, plasticizer and polymer, respectively. To synthesize these membranes, these 3 components were dissolved in the solvent tetrahydrofuran (THF). THF has a very low boiling point (66 °C, 151 °F) and was allowed to evaporate slowly over 24 hours. As described in Chapter 2, this process produces the flexible polymeric membranes that are later incorporated directly into ion-selective electrodes.

Direct determination of metalloporphyrins with gas chromatography is generally considered a difficult experiment, due to the high boiling points of the metalloporphyrins. For example, a study from Gallegos, et al., measured vanadium porphyrins in petrochemical materials using gas chromatography – mass spectrometry (GC-MS) at temperatures up to 350 °C.<sup>30</sup>

Two of the modern gas chromatography instruments in the Missouri State University Chemistry department were utilized to see if erbium(III) tetraphenylporphyrin could be characterized when dissolved in the solvent THF. As discussed in Chapter 1, gas chromatography is a method of separating the many chemical components of a mixed solution via their interactions with a stationary phase within a column. Under conditions described in Chapter 2, a solution of  $1.1 \times 10^{-4}$  M erbium(III) tetraphenylporphyrin in THF was prepared and measured using a Varian 430 gas chromatograph instrument with flame ionization detection. A

large solvent peak at approximately 1.0 minute was found, along with a smaller peak at 4.2 minutes and a larger peak at 4.4 minutes (see Figure 14). The chromatogram was allowed to run for ~30 minutes more and no other peaks were detected.

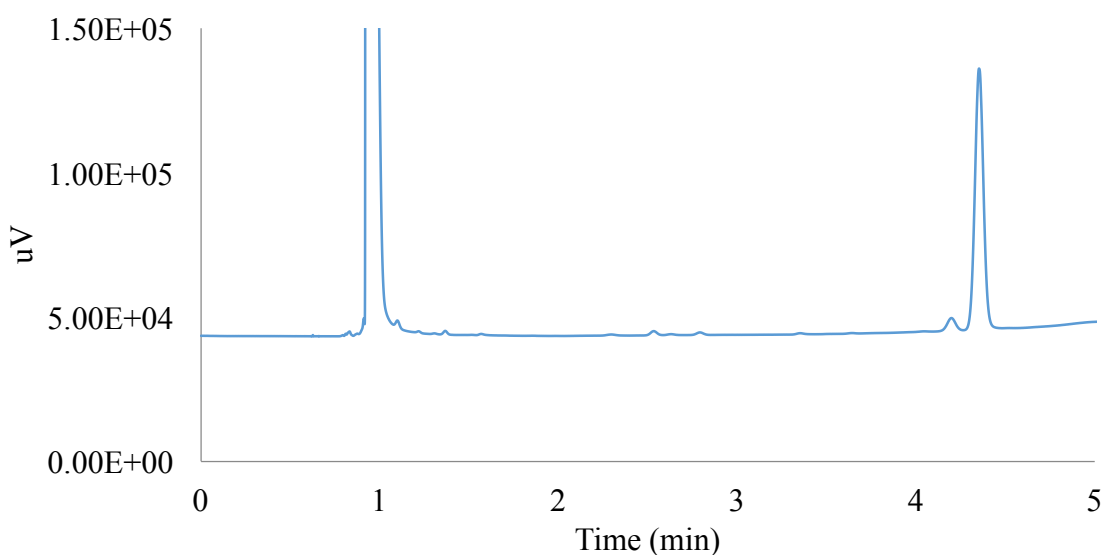


**Figure 14.** Initial chromatogram of the erbium (III) tetraphenylporphyrin solution in THF.

The solution of erbium(III) tetraphenylporphyrin and THF was allowed to sit in a dark cabinet for approximately one month after preparation. The freshly made solution was a bright pink-purple color and the older sample was a reddish-orange color (Figure 7). When the sample was measured again using the same parameters (Figure 15), the resulting chromatogram was slightly different than the previous one. The peak at 4.2 minutes was more prominent, and the peak at 4.4 minutes was smaller. A very small peak at around 4.1 minutes was now found as well.



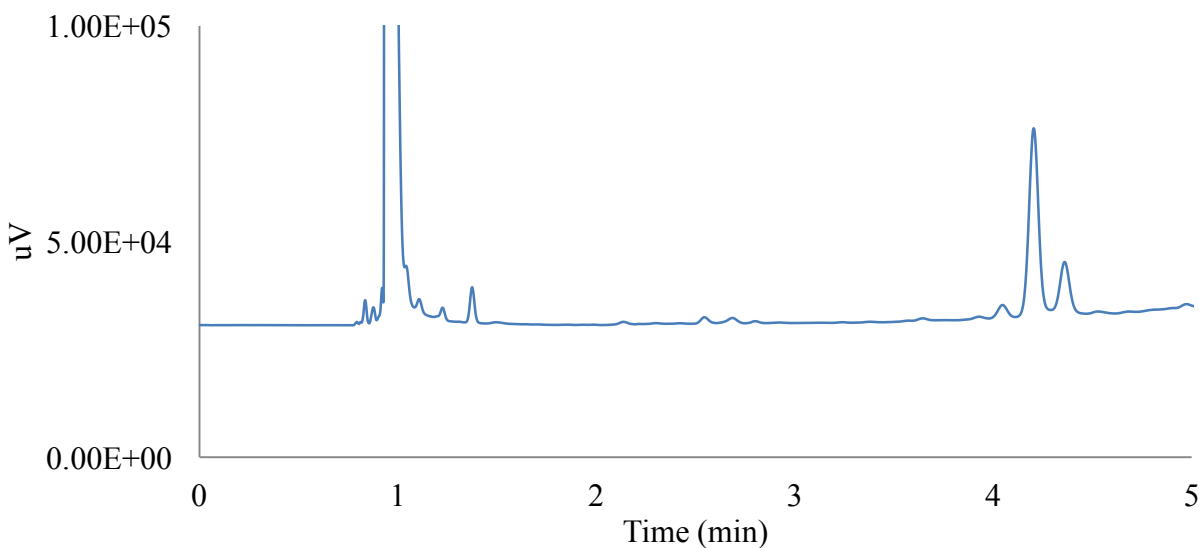


**Figure 15.** One-month old erbium (III) tetraphenylporphyrin solution in THF chromatogram.

Additional solutions were prepared to compare with those found previously with the metalloporphyrin and THF mixtures. A sample that contained only the THF solvent was examined via the GC instrument. Another solution that was prepared was the free (no metal) tetraphenylporphyrin ( $\text{H}_2\text{TPP}$ ) in THF. The last solution that was prepared was erbium(III) acetate hydrate,  $\text{Er(III)(acetate)}_3$  in THF. In all of these last three chromatograms (data not shown), peaks were found at nearly identical retention times as that of the first chromatogram (Figure 14), a large peak near 1.0 minute and two peaks at 4.2 and 4.4 minutes. This data will be discussed in Chapter 4.

### 3.2 Gas Chromatography Mass Spectrometry Analysis

In order to identify the components found in the previous gas chromatography experiments, another gas chromatography detector was employed. Gas chromatography-mass spectrometry (GC-MS) was chosen due to its ability to identify the chemical components that elute in the chromatogram. As discussed in Chapter 1, the mass spectrometer detector of the

instrument uses mass to charge ratios to identify compounds in a solution. GC-MS is also a more sensitive method of analysis that could potentially measure compounds that were not previously detectable on the gas chromatograph with a flame ionization detector. Much like the earlier technique, solutions were prepared and measured under similar conditions. A freshly made erbium(III) tetraphenylporphyrin / THF solution with  $1.1 \times 10^{-4}$  M concentration was prepared and measured. The chromatogram was similar to the data presented in the previous section, but the mass spectrometer was able to label the masses of the most prominent peaks as well as compare those results to the system library to identify the chemical compound (Figure 16).

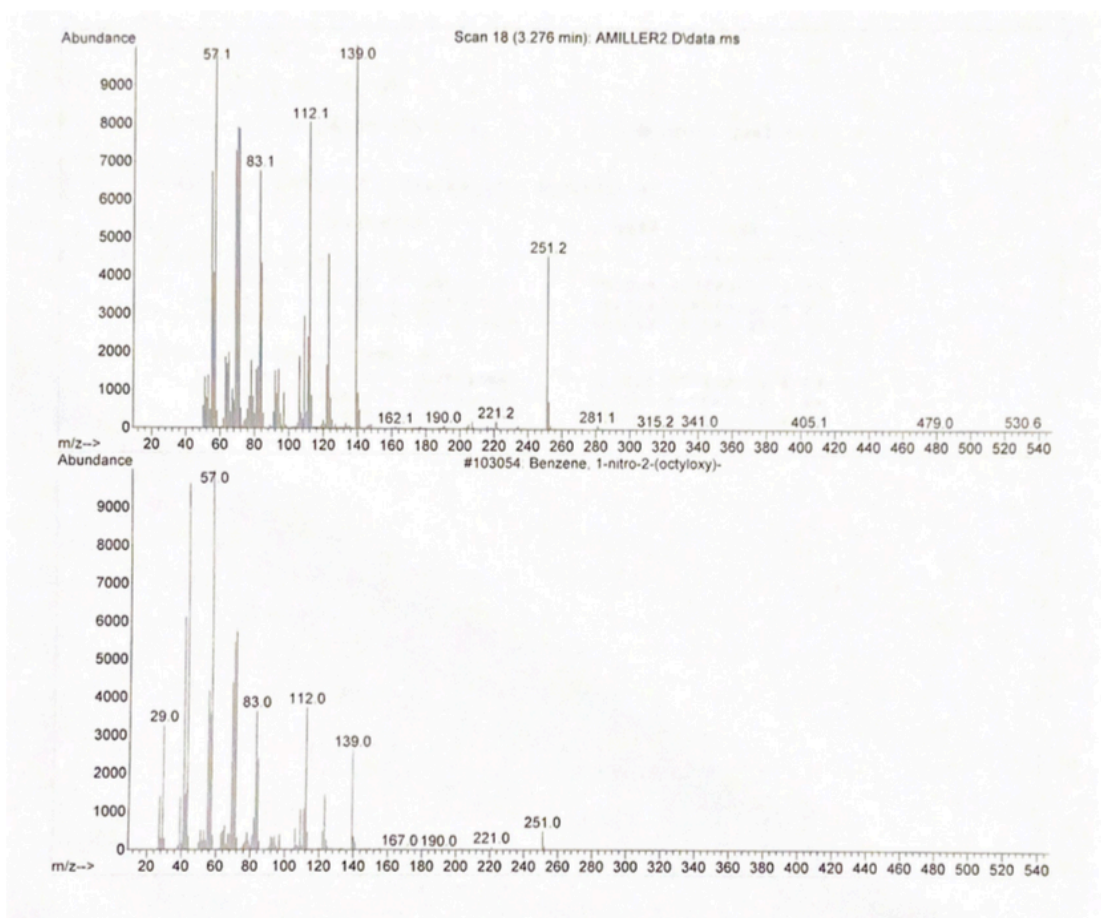


**Figure 16.** GC-MS results of (top) erbium (III) tetraphenylporphyrin and (bottom) the identified compound *o*-nitrophenyl octyl ether.

The instrument identified the compound as *ortho*-nitrophenyl octyl ether, which is the plasticizer used for the synthesis of the metalloporphyrin-based membranes. The two spectra appear to be identical, and the instrument labeled them with 95% quality, indicating the instrument has high confidence in the identity. The large percent quality suggests that the instrument was confident in its identification of the chemical compounds present in the solution. This chromatographic data will be discussed in Chapter 4.

### 3.3 UV-Visible Spectroscopy Analysis of Porphyrin Solutions

The first optical technique that was applied to the analysis of the metalloporphyrin was ultraviolet-visible (UV-Visible) spectroscopy using two different instruments. UV-Visible spectroscopy was chosen for the first set of optical measurements because it is a popular method of analysis of metalloporphyrins. As discussed in Chapter 1, metalloporphyrins are known to be very absorbing compounds in the ultraviolet and visible regions of the electromagnetic spectrum. UV-visible spectroscopy can be used in the qualitative and quantitative determination of many different compounds. With metalloporphyrins, UV-Visible spectroscopy can be utilized to determine whether monomers or dimers are present.

The initial analyses were of the various solutions including the erbium metal ( $\text{Er}^{3+}$ ), the free tetraphenylporphyrin ( $\text{H}_2\text{TPP}$ ) and erbium(III) tetraphenylporphyrin ( $\text{Er(III)TPP(acac)}$ ) in the THF solvent. The Agilent Cary 60 spectrophotometer was utilized for this experiment and the instrumental conditions are described in Chapter 2. The first sample that was measured was erbium(III) acetate hydrate in THF, which produced faint and indistinguishable absorbance in the visible region (data not shown). This eliminated the possibility of identifying the metal component of the porphyrin structure using this technique. The next sample was the free

tetraphenylporphyrin (H<sub>2</sub>TPP) in THF, which produced multiple peaks (Figure 17). The major peaks in the Q band region were at 513 nm, 546 nm, 590 nm, and 646 nm. There was also absorbance in the Soret band region around 400 nm that did not have differentiating peaks. The peaks that were present on the spectrum were indicative of a typical porphyrin compound regardless of the missing metal.<sup>31</sup> The last sample that was analyzed was the older discolored erbium(III) tetraphenylporphyrin solution in THF that was previously used in the gas chromatography experiments. The solution that was measured was Er(III)TPP(acac) in THF at a  $1.2 \times 10^{-4}$  M concentration, which also produced multiple peaks (also in Figure 17). The discolored solution was analyzed to identify the potential causes for the color change. There was a large, off-scale peak at around ~420 nm and a single band at 540 nm.

A freshly made  $1.1 \times 10^{-4}$  M erbium(III) tetraphenylporphyrin in THF solution was then measured. For this experiment, the Perkin Elmer Lambda 650 spectrophotometer was utilized, with the instrumental conditions described in Chapter 2. This spectrum indicated major absorption in the Soret band region at approximately 420 nm and in the Q band region at 481 nm, 514 nm, 555 nm, 593 nm, and 645 nm (Figure 18). The major absorption peaks were indicative of a typical metalloporphyrin complex. Both the Cary and Perkin Elmer instruments appear to be satisfactory for these experiments. The Perkin Elmer instrument is a double monochromator system and allows measurements of absorbance at higher levels than the Cary single monochromator system (compare Figures 17 and 18), which improved the appearance of the Soret band at 420-425 nanometers. However, at lower metalloporphyrin concentrations with lower absorbance values, either spectrophotometer would work equally well.

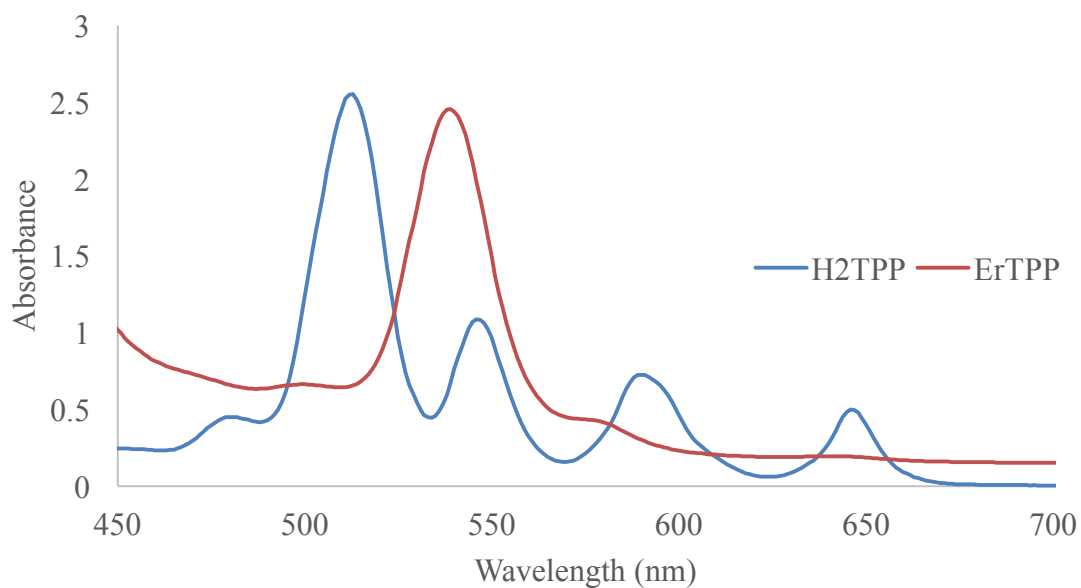
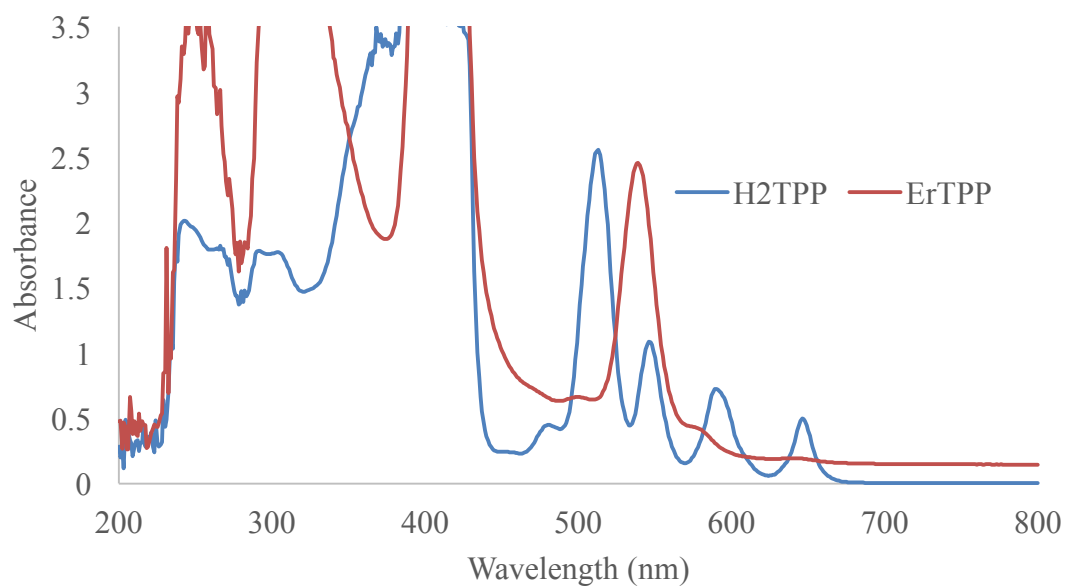


**Figure 17.** (top) UV-Visible spectra of free tetraphenylporphyrin (H<sub>2</sub>TPP) and erbium (III) tetraphenylporphyrin in THF (bottom) spectra of the solutions from 450 to 700 nanometers.

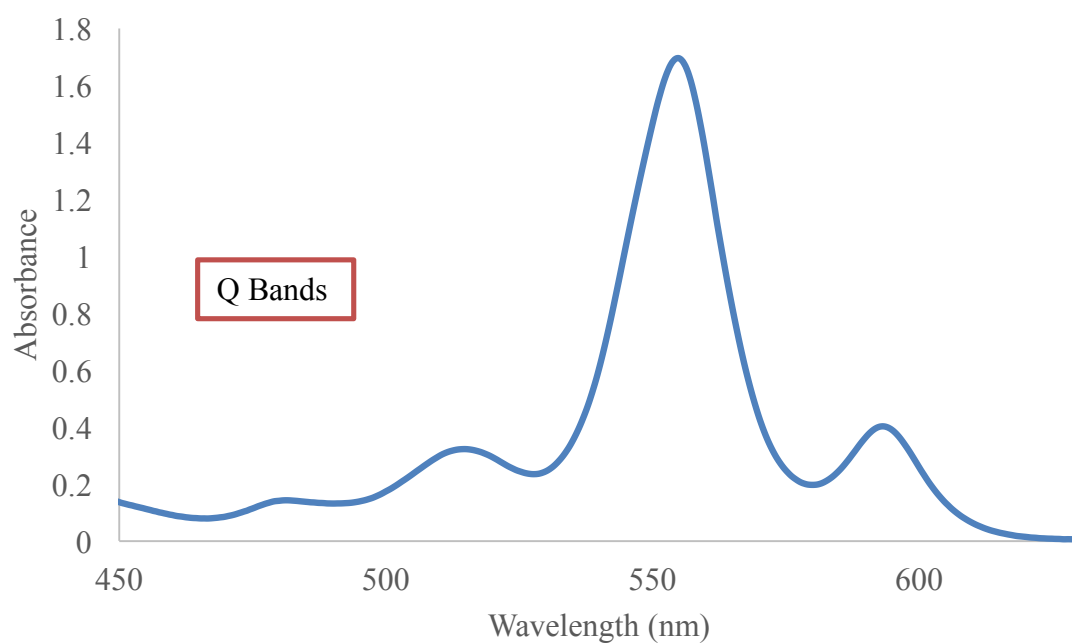
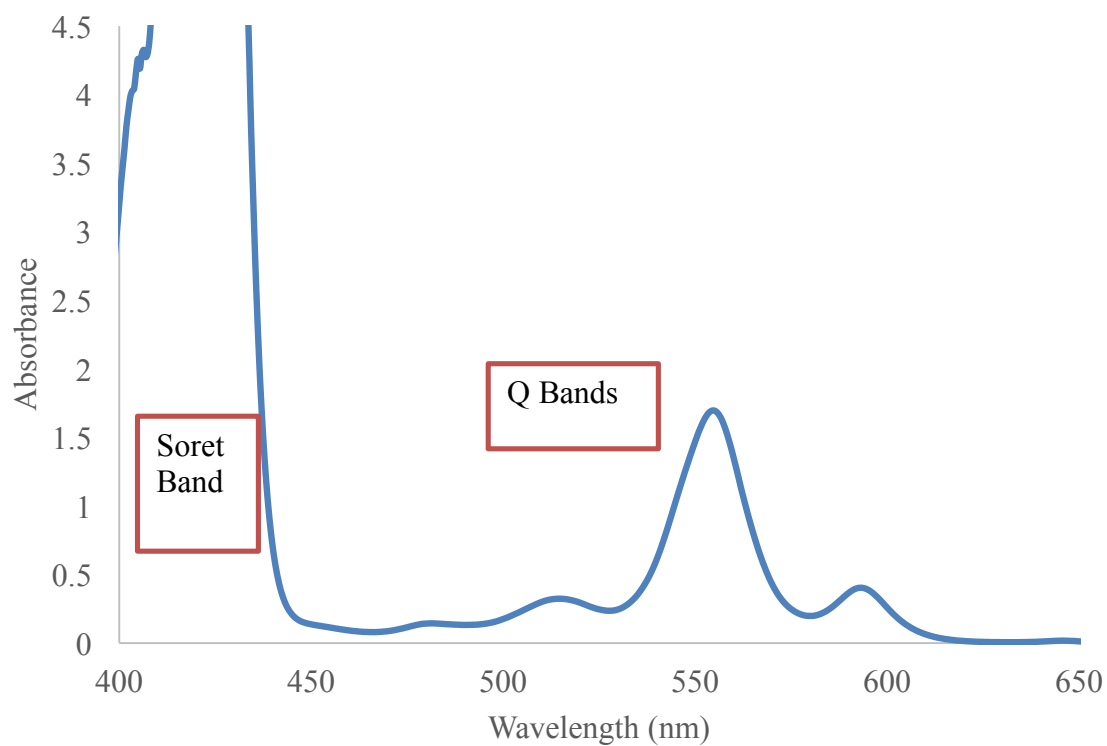


**Figure 18.** (top) UV-Visible spectrum of erbium (III) tetraphenylporphyrin in THF and (bottom) Zoomed in spectrum of Q band region.

### 3.4 UV-Visible Spectroscopy Analysis of Metalloporphyrin-Based Membranes

The next step of this work was the determination of the optical properties of the same metalloporphyrin-based membrane that are used in the potentiometric ion-selective electrode studies. Understanding the membrane and solution interface reactions has the potential to describe how the metalloporphyrin is interacting with the target anions. The buffers that were analyzed for this technique are solutions are frequently used for the ion selective electrode experiments. It was important to observe the interactions and how they changed in different concentrations. To understand the membrane interactions, a membrane was prepared for analysis rather than a liquid solution of the porphyrin compound. In the membranes, the porphyrin compound is very dilute and is incorporated with PVC and *o*-NPOE plasticizers. As described in Chapter 2, a membrane film was synthesized for these analyses and was measured in different standard sodium benzoate solutions. These thin films were cast onto glass slides and inserted into cuvettes, either dry or filled with buffer and sodium benzoate solutions.

The first membrane film (designated A in Figure 19) produced a slightly noisy absorption spectrum when measured under dry conditions (before exposure to the buffer and sodium benzoate aqueous solutions). The maximum absorption wavelength for the first membrane under dry conditions was approximately 423 nm, which correlates to the ultraviolet-visible data from the Er(III)(TPP) / THF data from the previous section. The bands in Q band region (450-700 nm) were very small (data not shown). Since the only major peak was present in the Soret band region, the scope was narrowed down to that specific region to observe the changes occurring to the membrane film in various solutions.

The polymer film-coated glass slide was then placed in a cuvette containing 0.05M N-morpholino ethanesulfonic acid (MES), buffered at pH 5.5. The film was allowed to equilibrate

in this aqueous solution for 10 minutes before measurement with the Cary 60 spectrophotometer. Standard solutions of sodium benzoate were prepared using the same MES buffer as the solvent. The optical film would also equilibrate in the sodium benzoate solutions for 10 minutes prior to measurement.

The baselines of the absorbance spectra appeared to be dependent on the placement of the coated glass slide within the cuvette. To better compare the different spectra, the absorbance values were normalized at 470 nanometers. As shown in Figure 19, the results of the first membrane did not indicate a major change in absorbance upon exposure to the 0.05M MES buffer or the sodium benzoate solutions ranging from  $10^{-5}$  to  $10^{-2}$  M.

The second membrane film (B) produced a much cleaner absorption peak for the dry membrane, however, it did appear to have a slightly larger absorbance than the first membrane (Figure 20). The change in absorbance values is likely due to the possibility of inconsistencies that were present in the preparation of the different membrane films. Each membrane film was hand made and had potential for some human error as well as inconsistencies in membrane solutions. Although there were slight differences in absorbance values, the major absorption peaks were also present in the Soret band region. The maximum absorption wavelength for the second membrane was approximately 420 nm, which was very close to the first membrane's results. The results of the second membrane did not indicate a major change in absorbance in the different buffer solutions (Figure 20). The spectra for the second membrane film were also normalized to allow for better comparison of the major absorption peak. Much like the first membrane film, there did not appear to be any significant changes that occurred to the absorbance of the membrane. The membrane films appeared to be sticking to the same trend regardless of the concentration of the buffer solutions.



The third membrane film (C) also produced a fairly clean spectrum for the dry membrane, however, it had slightly larger absorbance values than the previous membranes (Figure 21). Again, this is likely due to inconsistencies in the membrane film preparation that could not be controlled. Although the absorbance values were on a different scale, the major absorption peak was once again present in the Soret band region. The maximum absorption wavelength was approximately 419 nm, which is very close to the other membrane films (Figure 21). The absorbance of the third membrane film also did not appear to significantly change in the various buffer solutions. The changes in concentration of the sodium benzoate did not cause a significant change in the major absorption peak. The spectra of the third membrane were also normalized to allow for a more accurate comparison between the different runs.

Once all three membrane films were measured in the different buffer solutions, the results were compared to determine the reproducibility of the analyses. The three membrane films did produce slightly unique results, however, all of them produced similar maximum absorption wavelengths between 419-423 nm (Figure 22). The spectra from the three membranes were averaged to allow for a better comparison of the major peak present (Figure 22). These precise results indicate the porphyrin membrane did not significantly change under various reaction conditions as well as unique sample preparation. There was only one major absorption peak for the three membranes in all of the buffer solutions. The consistency in the peak suggested there were not any changes occurring in the porphyrin membrane. Some studies have noted apparent aggregation that occurs within the porphyrin molecule in various chemical conditions.<sup>20,32</sup> However, the aggregation usually causes a shift in the major absorption peak by approximately 20 nm.<sup>9</sup> In this particular experiment, there were not significant changes in the major absorption wavelength that would suggest any aggregation within the molecule. Rather than forming the

two conformations, monomer and dimer, of the porphyrin complex, it appears the erbium porphyrin compound remained at equilibrium in the solution.

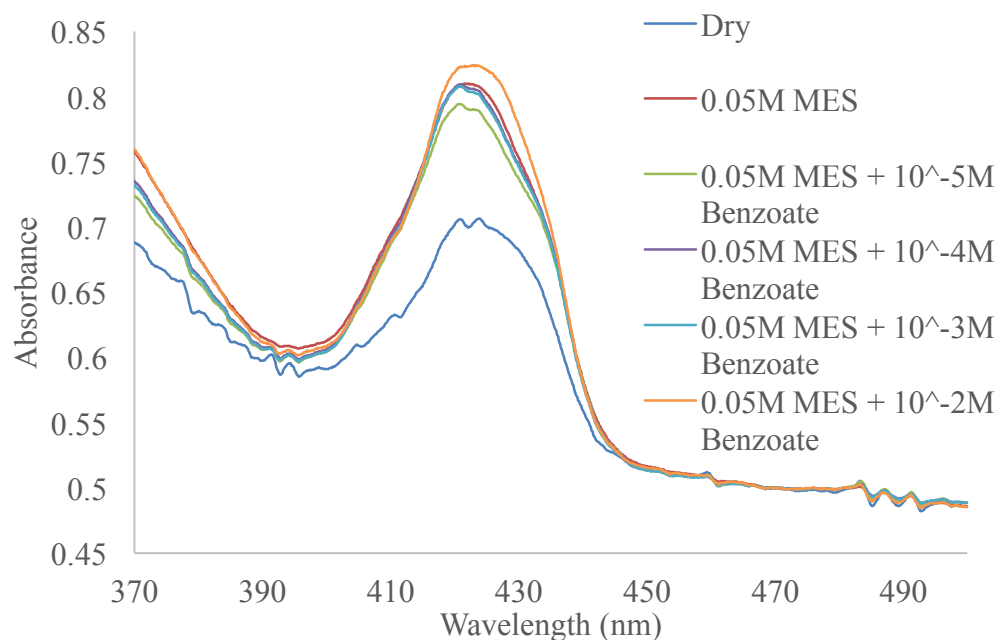


**Figure 19.** Membrane film A absorbance spectra in various aqueous solutions.

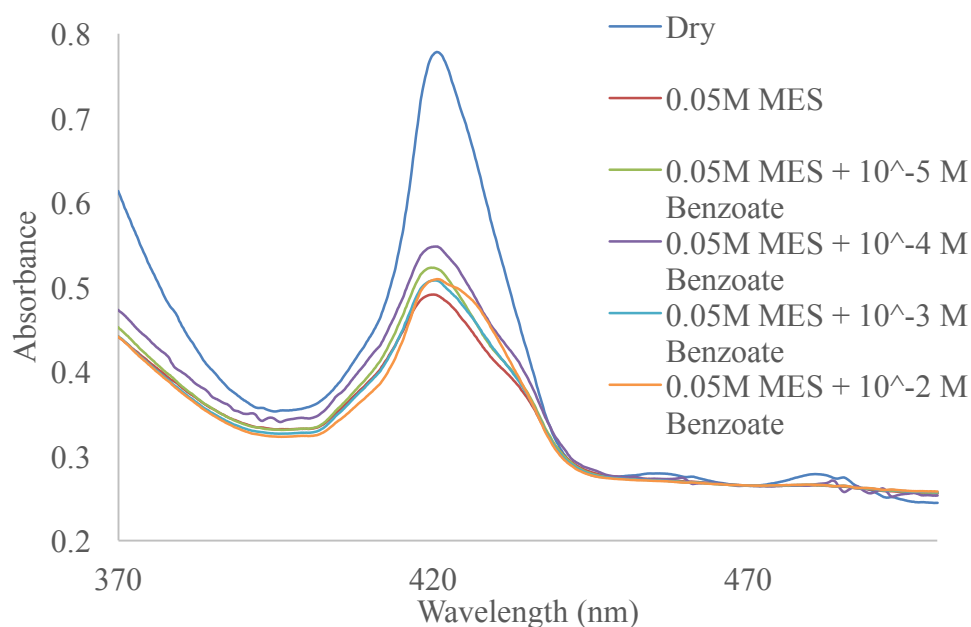


**Figure 20.** Membrane film B absorbance spectra in various aqueous solutions.

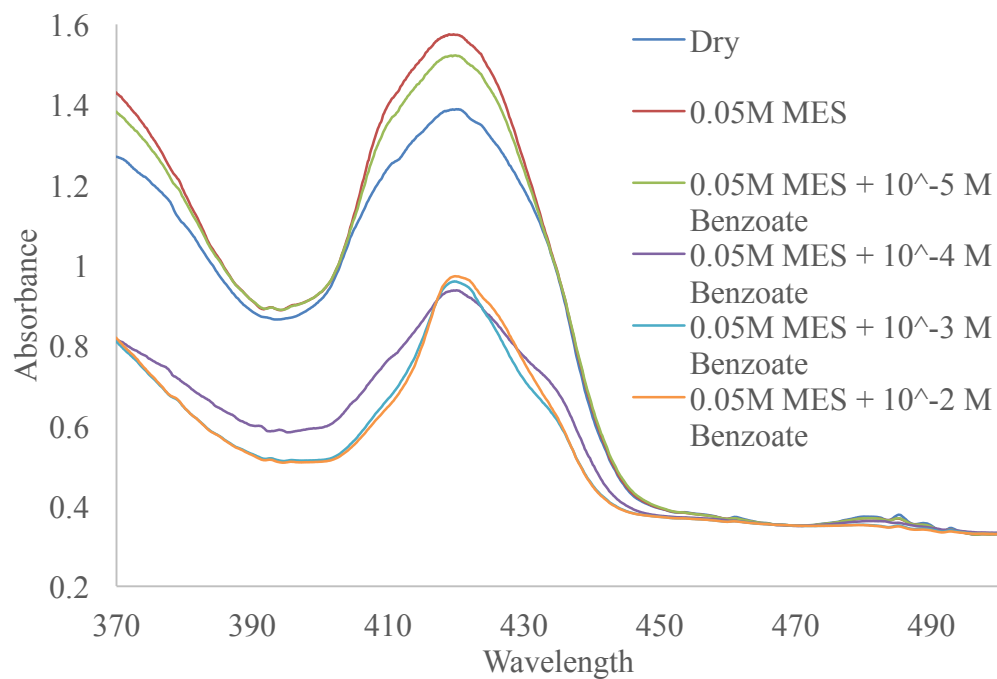


**Figure 21.** Membrane film C absorbance spectra in various aqueous solutions.

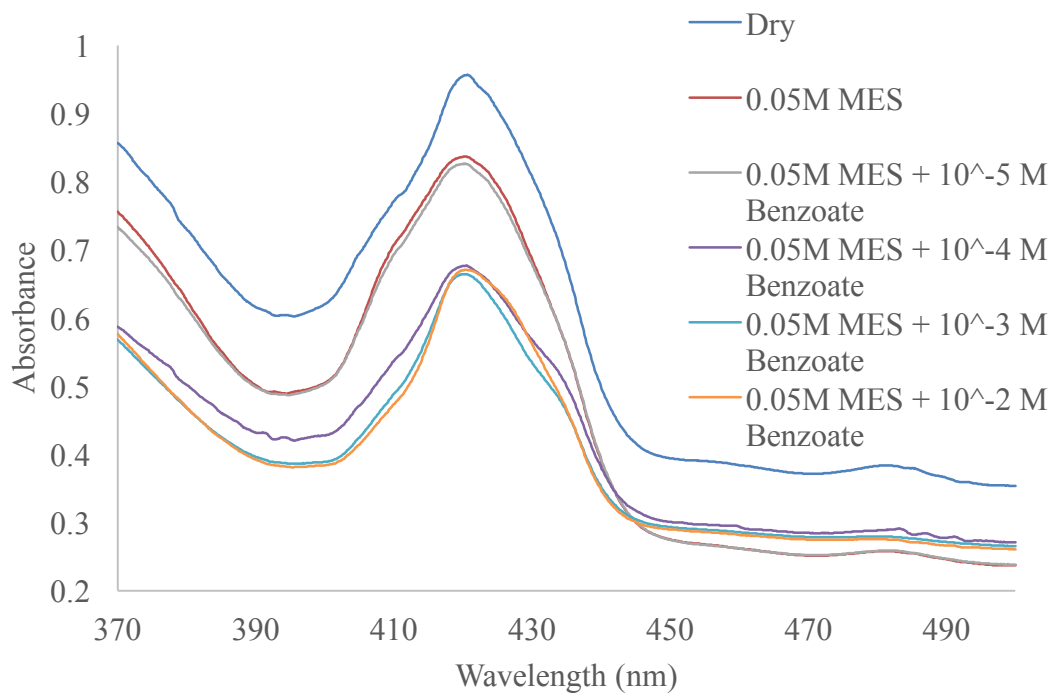


**Figure 22.** Membrane films A-C average absorbance spectra in various aqueous solutions.

### 3.5 Fluorescence Spectroscopy Analysis

The last optical technique that was used in the investigations of erbium(III) tetraphenylporphyrin was fluorescence spectroscopy. Since porphyrin compounds are known to absorb easily in the ultraviolet and visible regions, the compound's ability to be observed using fluorescence was investigated. As discussed in Chapter 1, fluorescence spectroscopy is a method of analysis that is significantly more sensitive than absorption spectroscopy as long as the compound has the ability to undergo the fluorescence process. Identifying the fluorescent properties of the porphyrin is the last aspect to understanding the optical properties of the compound. The solution that was prepared for gas chromatography-mass spectrometry experiments was also used for these measurements. The major absorption wavelengths that were observed in the previous optical technique were also used as a starting point for these analyses. The first major absorption peak using UV-visible spectroscopy was around 420 nm, so a starting excitation wavelength of 420 nm was used. The initial slit widths that were used were 2.5 nm, but the amount of noise that was present on the spectra made it difficult to identify the emission peaks. The slit widths were then increased to 10.0 nm and the results were significantly clearer and more precise. The major emission peaks that were present on the first spectrum were at approximately 650 nm and 720 nm (Figure 23). There was also a major peak at 420 nm, but it was likely due to the excitation light. The peaks that were present were quite clear and had little noise. For the next run, another major absorption wavelength that was present in UV-visible spectroscopy was chosen, which was 480 nm. The same slit widths were incorporated due to the clear noise deduction. This spectrum indicated a few more emission peaks were present. The notable peaks were at 530 nm, 583 nm, 656 nm, and 721 nm (Figure 24). Another peak at 488 nm was also present, but it was likely due to the excitation light.

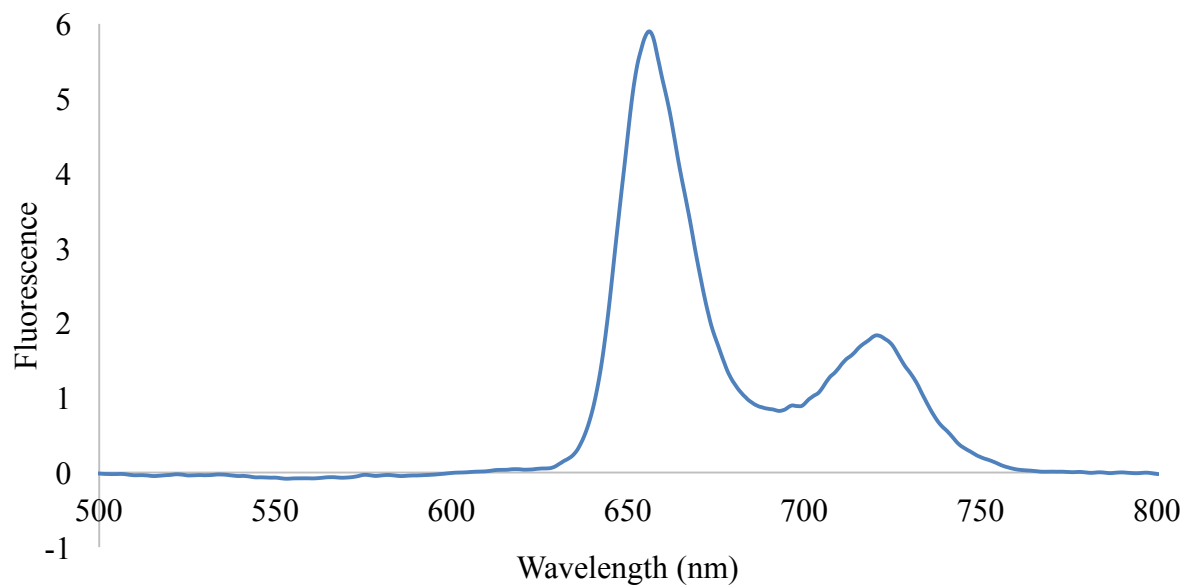


**Figure 23.** Fluorescence spectrum at 420 nm excitation wavelength.

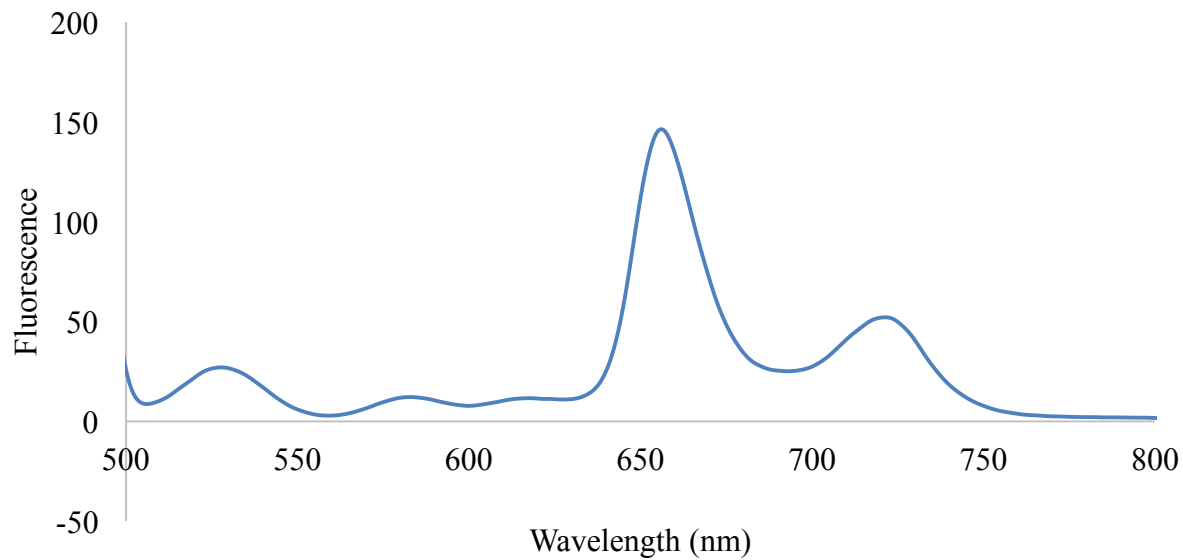


**Figure 24.** Fluorescence spectrum at 480 nm excitation wavelength.

## CHAPTER IV. DISCUSSION

### 4.1 Gas Chromatography

The resulting chromatograms of the metalloporphyrin / THF solutions indicated the major peaks were not from the porphyrin complex, but rather from another component of the solution (Figure 14 and 15). When the chromatogram was compared to the known retention times of pure THF, it was concluded that the eluting components were from the solvent rather than the porphyrin structure. Due to the extremely large molecular weight of erbium(III) tetraphenylporphyrin, it was suspected the boiling point may not be reached using this particular instrument, thus, potentially the compound would not be seen eluting off the column. This led to the investigation using another chromatographic technique.

### 4.2 Gas Chromatography Mass Spectrometry

The mass spectrometry addition to gas chromatography provided the ability to identify the chemical compounds that eluted off the column and produced major peaks. From the analysis of the erbium(III) tetraphenylporphyrin solution, the instrument was able to compare the resulting chromatogram to other molecules in its library of chemicals. The instrument identified the chemical components of the chromatogram as *ortho*-nitrophenyl octyl ether, which is the plasticizer that is used in the preparation of the metalloporphyrin-based polymer membranes (Figure 16). However, these results were unexpected since the solution, in theory, should not have contained the plasticizer. The solution that was prepared and measured only contained the erbium(III) tetraphenylporphyrin and THF. The source of the *o*-NPOE in the THF was not investigated further, but a possible source of contamination could have been from the lab itself,

as *o*-NPOE is one of the most often used membrane components in the Steinle laboratory. It is possible that a glass pipette at the balance to weigh out the *o*-NPOE (a liquid at room temperature) was later accidentally used in the container of THF. To confirm this suspicion, a fresh bottle of THF could be obtained and examined via GC-MS under the same instrumental conditions.

As chromatographic techniques did not provide a strong method for characterizing the metalloporphyrin within the THF solvent, it was decided to investigate spectroscopic techniques since metalloporphyrins are known to have unique optical properties.

#### **4.3 UV-Visible Spectroscopy of Porphyrin Solutions**

The first spectroscopic technique that was explored involved the analysis of the erbium(III) tetraphenylporphyrin solution as well as various other solutions of the chemical components of the metalloporphyrin. The free tetraphenylporphyrin ( $H_2TPP$ ), erbium(III) acetate hydrate, and pure THF solutions allowed the comparison of the absorption wavelengths to erbium(III) tetraphenylporphyrin to determine whether the compound was dissociating over time into its chemical components. The porphyrin solution that had changed color over time was also measured to determine whether a structural change had occurred. The older porphyrin solution that had undergone a slight color change produced similar results to the fresh solution with a single absorption peak in the Q band region. The tetraphenylporphyrin ( $H_2TPP$ ) / THF solution was compared to the erbium(III) porphyrin solution and the changes in the Q band region between the two solutions were measured (Figure 17). The resulting spectra were different, as the erbium porphyrin solution absorbed in one major peak rather than the four peaks typical of free porphyrin structure (Figure 17). Overall, the results of the different solutions indicated the

erbium(III) porphyrin remained structurally intact after a month in solution, however, the color change that occurred could be indicative of some instability of the solutions. For example, the THF solvent may have been older, which created a slightly unstable solution.

Using a freshly made erbium(III) porphyrin / THF solution, the Soret and Q bands absorption wavelengths were precisely quantified. The newly-made metalloporphyrin solution presented typical results for a metalloporphyrin compound (Figure 18).<sup>1,17,26,27,28</sup> There was one major Soret band and four major Q bands, which was expected with the analysis of the erbium(III) tetraphenylporphyrin (Figure 18). The spectroscopic results help describe the optical properties of the erbium porphyrin complex. Once the optical properties of the porphyrin compound were quantified, the optical thin film studies were planned using ultraviolet-visible spectroscopy.

#### **4.4 UV-Visible Spectroscopy of Metalloporphyrin-Based Membranes**

The synthesis of the porphyrin membrane film was vital to the analysis of the reactivity of the erbium(III) tetraphenylporphyrin within the film. The goal was to better understand the interface reactions that occurred between the membrane and different solutions. With the membrane film, the absorbance of radiation within the visible part of the electromagnetic spectrum was determined. A “dry” membrane prior to exposure to aqueous solutions was examined, as well as after exposure to a pH-buffered solution and increasing concentrations of sodium benzoate. Sodium benzoate was chosen because the ion-selective electrodes have shown an affinity for the benzoate anion in potentiometric studies. Three replicate erbium(III) tetraphenylporphyrin-based membrane films produced a major absorption peak in the Soret band region, but the bands in the Q bands region were too low to be measured accurately. This is



likely due to the low concentrations of the erbium(III) tetraphenylporphyrin compound in the membrane that was prepared, as opposed to the solution-phase experiments where the concentrations were significantly higher. Since the major absorption peak present was in the Soret bands region, the scope of the spectra focused on the wavelength range of 370-500 nm. The Soret band is a porphyrin ligand centered absorbance band influenced by the substitution pattern, therefore, it is not likely impacted by the erbium(III) metal center. The major absorption wavelengths for the three membrane films ranged from 419-423 nm, which suggested the experiments were highly reproducible regardless of the possible inconsistencies in the preparation of the film (Figure 19, 20, 21, and 22). Overall, each run was very precise and appeared to remain consistent in the different buffer solutions. The changes in concentration of the sodium benzoate in the MES buffer solutions did not appear to alter the absorbance of the metalloporphyrin-based membrane (Figure 19, 20, 21, and 22). The results indicated the properties and the structure of the erbium metalloporphyrin compound remained constant. There did not appear to be any aggregation or dimerization occurring within the porphyrin complex. Some past research has found that some metalloporphyrins can produce two conformers of the porphyrin structure including the monomer and the dimer, which has been known to occur in certain solvents including highly concentrated buffers.<sup>1,32</sup> This aggregation occurs between the  $\pi$  orbitals of the porphyrin structure due to the close proximity to each other in solution.<sup>8,32</sup> The aggregation and the dimerization of porphyrin compounds depend on the solution's characteristics including the ionic strength of both the lipophilic agent and the ligands as well as the solvent composition.<sup>1,20</sup> Both of these factors can lead to a shift in peaks in the Soret band region. Although this phenomenon has been found in other previous ion-selective electrodes involving metalloporphyrins,<sup>9</sup> it was not found in these experiments. The erbium(III)

tetraphenylporphyrin structure appeared to remain in a monomeric in all of the buffer solutions. The results suggested the erbium(III) tetraphenylporphyrin within the polymeric film is not likely to undergo aggregation under the conditions used for the ion-selective electrodes, therefore, a monomeric response mechanism is likely to be prevalent.

#### **4.5 Fluorescence Spectroscopy**

The last optical technique that was applied to the analysis of erbium(III) tetraphenylporphyrin was fluorescence spectroscopy. The first excitation wavelength that was used was 420 nm and the two major emission peaks were very clear and lacked significant noise (Figure 23). The two major peaks were at 650 nm and 720 nm (Figure 23). These results were then compared to previous research that had been performed on similar compounds under similar conditions. It appeared that the chosen excitation wavelength agreed with previous methods of analysis.<sup>26</sup> The two peaks also appeared to align with the results of multiple other researchers.<sup>17,26,33</sup> Overall, tetraphenylporphyrin compounds were observed to fluoresce in the Q band region around 650 nm and 720 nm.<sup>17,26,33</sup> With these fluorescence results, more unique optical properties of erbium(III) tetraphenylporphyrin were again quantified.

## CHAPTER V. CONCLUSION AND FUTURE WORK

The chromatographic techniques did not provide additional information regarding the reactivity or chemical characteristics of the porphyrin compound. However, it was determined chromatography was not an ideal method of analysis. A molecule (*o*-NPOE) that should have not been present within the erbium porphyrin or the THF solution was found in the mass spectrometry data (Figure 16). Future experiments with new solvents from the manufacturer could help solve this question. The spectroscopic techniques did provide unique optical properties including the absorption and fluorescence emission wavelengths of the porphyrin structure in the ultraviolet visible light region. The prominent optical properties including the colorful nature of the erbium(III) tetraphenylporphyrin compound are largely due to the highly conjugated properties of the porphyrin structure. It was also confirmed that the porphyrin structure was not dissociating over time in the THF solvent, which is an important piece of knowledge since the electrode membranes are constructed in THF (Figure 17). The reactivity of the metalloporphyrin structure within the polymeric film was also quantified and revealed there was not any aggregation or dimerization that occurred under these specific reaction conditions using the erbium porphyrin compound (Figure 22). The lack of aggregation suggested the erbium porphyrin compound is not likely to undergo any structural changes that could interfere with potential ion selective electrode measurements. Overall, many characteristics and properties of the erbium(III) tetraphenylporphyrin were identified using various analytical techniques.

In the future, the plan is to continue to investigate the spectroscopic techniques that can be used to describe erbium(III) tetraphenylporphyrin. Specifically, the plan is to further investigate the fluorescence of the porphyrin complex since prominent emission wavelengths

were observed. Optimizing the parameters for the fluorescence of the porphyrin compound would allow the optical properties of the porphyrin structure to be better quantified. The fluorescent properties also could lead to more projects investigating the potential use of porphyrin compounds in fluorescent indicators for specific ions, much like the ion selective electrodes that are currently used. The goal is to expand the knowledge of the porphyrin's reactivity to improve the sensitivity and selectivity of ion selective electrodes.

## REFERENCES

- (1) Giovannetti, R. The Use of Spectrophotometry UV-Vis for the Study of Porphyrins. In *Macro to Nano Spectroscopy*; Uddin, Dr. J., Ed.; InTech, **2012**; pp 87-108.
- (2) Sen, P.; Hirel, C.; Andraud, C.; Aronica, C.; Bretonnière, Y.; Mohammed, A.; Ågren, H.; Minaev, B.; Minaeva, V.; Baryshnikov, G.; Lee, H.; Duboisset, J.; Lindgren, M. Fluorescence and FTIR Spectra Analysis of Trans-A<sub>2</sub>B<sub>2</sub>- Substituted Di- and Tetra-Phenyl Porphyrins. *Materials* **2010**, 3(8), 4446-4475.
- (3) Barbe, J. M.; Ratti, C.; Richard, P.; Lecomte, C.; Gerardin, R.; Guillard, R. Tin (II) Porphyrins: Synthesis and Spectroscopic Properties of a Series of Divalent Tin Porphyrins. X-ray Crystal Structure of (2,3,7,8,12,13,17,18-Octaethylporphinato)tin(II). *Inorg. Chem.* **1990**, 29(20), 4126-4130.
- (4) Vlascici, D.; Plesu, N.; Fagadar-Cosma, G.; Lascu, A.; Petric, M.; Crisan, M.; Fagadar-Cosma, E. Potentiometric Sensors for Iodide and Bromide Based on Pt(II)-Porphyrin. *Sensors* **2018**, 18(7), 1-18.
- (5) Bakker, E.; Bühlmann, P.; Pretsch, E. Carrier-Based Ion Selective Electrodes and Bulk Optodes General Characteristics. *Chem. Rev.* **1997**, 97(8), 3083-3132.
- (6) Al-Shewiki, R.; Mende, C.; Buschbeck, R.; Siles, P.; Schmidt, O.; Rüffer, T.; Lang, H. Synthesis, Spectroscopic Characterization and Thermogravimetric Analysis of Two Series of Substituted (Metallo)tetraphenylporphyrins. *Beilstein J. Nanotechnol.* **2017**, 8(1), 1191-1204.
- (7) Röckert, M.; Franke, M.; Tariq, Q.; Lungerich, D.; Jux, N.; Stark, M.; Kaftan, A.; Ditze, S.; Marbach, H.; Laurin, M.; Libuda, J.; Steinruck, H.; Lytken, O. Insights in Reaction Mechanistics: Isotopic Exchange during the Metalation of Deuterated Tetraphenyl-21, 23D-Porphyrin on Cu(111). *J. Phys. Chem. C* **2014**, 118(46), 26729-26736.
- (8) Wang, Y.; Sauriat-Dorizon, H.; Korri-Youssofi, H. Direct Electrochemical DNA Biosensor Based on Reduced Graphene Oxide and Metalloporphyrin Nanocomposite. *Sensors and Actuators B* **2017**, 251, 40-48.
- (9) Steinle, E.D; Amemiya, S.; Meyerhoff, M. E. Origin of Non-Nernstian Anion Response Slopes of Metalloporphyrin-Based Liquid/Polymer Membrane Electrodes. *Anal. Chem.* **2000**, 72(23), 5766-5773.
- (10) Witowska-Jarosz, J.; Górski, L.; Malinowska, E.; Jarosz, M. Mass Spectrometric Investigation of Gallium and Zirconium Complexes with Octaethylporphyrin and Tetraphenylporphyrin. *J. Mass. Spectrom.* **2002**, 37(12), 1236-1241.

- (11) Steinle, E. D.; Schaller, U.; Meyerhoff, M. E. Response Characteristics of Anion-Selective Polymer Membrane Electrodes Based on Gallium(III), Indium(III) and Thallium(III) Porphyrins. *Anal. Sci.* **1998**, *14*(1), 79-84.
- (12) Toganon, M.; Furata, H. N-Fused Porphyrin: A Maverick Member of the Porphyrin Family. *Chem. Lett.* **2019**, *48*, 615-622.
- (13) Furata, H.; Ishizuka, T.; Osuka, A.; Dejima, H.; Nakagawa, H.; Ishikawa, Y. NH Tautomerism of N-Confused Porphyrin. *J. Am. Chem. Soc.* **2001**, *123*(25), 6207-6208.
- (14) Geier, G. R., III; Haynes, D. M.; Lindsey, J. S. An Efficient One-Flask Synthesis of N-Confused Tetraphenylporphyrin. *Org. Lett.* **1999**, *1*(9), 1455-1458.
- (15) Kadish, K. M.; Caemelbecke, E. V. Electrochemistry of Metalloporphyrins in Nonaqueous Media. *Encyclopedia of Electrochemistry, Bioelectrochemistry*; Wilson, G. S., Ed.; Wiley-VCH: Weinheim, Germany, 2002; Vol 9, pp 175-228.
- (16) Messick, M. S.; Kishnan, S. K.; Hulvey, M. K.; Steinle, E. D. Development of Anion Selective Polymer Membrane Electrodes Based on Lutetium (III) Porphyrins. *Anal. Chim. Acta* **2005**, *539*(1-2), 223-228.
- (17) Semenishyn, N. N.; Smola, S. S.; Rusakova, N. V.; Martynov, A. G.; Birin, K. P.; Gorbunova, Y. G.; Tsivadze, A. Y. Infrared 4f-Luminescence of Erbium(III) Complexes with Tetrapyrrole Ligands. *Macroheterocycles* **2018**, *11*(3), 262-268.
- (18) Pizzoferrato, R.; Lagonigro, L.; Ziller, T.; Carlo, A. D.; Paolesse, R.; Mandoj, F.; Ricci, A.; Sterzo, C. L. "Förster energy transfer from poly(arylene-ethynylene)s to an erbium-porphyrin complex," *Science Direct* **2004**, *300* (1-3), 217-225.
- (19) Lisak, G.; Tamaki, T.; Ogawa, T. Dualism of Sensitivity and Selectivity of Porphyrin Dimers in Electroanalysis. *Anal. Chem.* **2017**, *89*(7), 3943-3951.
- (20) Avlasevich, Y. S.; Rat'ko, A. A.; Egorov, V. V. Change in the Absorption Spectra of Membranes Containing Co(III)- and Sn(IV) Tetraphenylporphyrins as a Result of the Use of Anion-Selective Electrodes Based on Them. *J. Appl. Spectrosc.* **2002**, *69*(4), 554-559.
- (21) Fujita, Y.; Kato, R.; Sawada, K.; Hattori, T. Two Dimensional Array Chloride Ion Image Sensor. *The Inorgo Conference 2018*, **2019**, 2067, 020014-1-020014-6.
- (22) Bakker, E.; Malinowska, E.; Schiller, R.; Meyerhoff, M. E. Anion-Selective Membrane Electrodes Based on Metalloporphyrins: The Influence of Lipophilic Anionic and Cationic Sites on Potentiometric Selectivity. *Talanta* **1994**, *41*(6), 881-890.
- (23) Skoog, D. A.; Holler, F. J.; Crouch, S. R. *Principles of Instrumental Analysis*, 7<sup>th</sup> ed.; Cengage Learning: Boston, MA, 2018.

- (24) Górski, L.; Meyerhoff, M.; Malinowska, E. Polymeric Membrane Electrodes with Enhanced Fluoride Selectivity Using Zr(IV)- Porphyrins Functioning as Neutral Carriers. *Talanta* **2004**, 63(1), 101-107.
- (25) Laba, K.; Lapkowski, M.; Officer, D. L.; Wagner, P.; Data, P. Electrochemical and Optical Aspects of Cobalt Meso-Carbazole Substituted Porphyrin Complexes. *Electrochim. Acta* **2020**, 330, 1-11.
- (26) Tao, S.; Li, G.; Zhu, H. Metalloporphyrins as Sensing Elements for the Rapid Detection of Trace TNT Vapor. *J. Mater. Chem.* **2006**, 16(46), 4521-4528.
- (27) Zhao, T.; Zhang, J.; Yang, X.; Xu, Q.; Lan, G. Synthesis and Structural Characterizations of Meso-Tetraphenylporphyrin. *Asian J. Chem.* **2014**, 26(10), 3050-3052.
- (28) Anjali, K.; Aswini, M.; Aswin, P.; Ganesh, V.; Sakthivel, A. Iridium Tetra(4-carboxyphenyl) Porphyrin, Calix[4]pyrrole and Tetraphenylporphyrin Complexes as Potential Hydrogenation Catalysts. *Eur. J. Inorg. Chem.* **2019**, 4087-4094.
- (29) Kadish, K. M.; D'Souza, F. D.; Villard, A.; Autret, M.; Caemelbecke, E. V.; Bianco, P.; Antonini, A.; Tagliatesta, P. Effect of Porphyrin Ring Distortion on Redox Potentials of  $\pi$ -Brominated-Pyrrole Iron (III) Tetraphenylporphyrins. *Inorg. Chem.* **1994**, 33, 5169-5170.
- (30) Gallegos, E. J.; Fetzer, J. C. High-Temperature GC/MS Characterization of Porphyrins and High Molecular Weight Saturated Hydrocarbons. *Energy & Fuels* **1991**, 5(3), 376-381.
- (31) Brazier, J. S. Analysis of the Porphyrin Content of Fluorescent Pus by Absorption Spectrophotometry and High Performance Liquid Chromatography. *J. Med. Microbiol.* **1990**, 33(1), 29-34.
- (32) Gerasimchuk, N. N.; Mokhir, A. A.; Rodgers, K. R. Synthesis and Characterization of Dimeric Mutually Coordinated Magnesium meso-2-Pyridylporphyrins. *Inorg. Chem.* **1998**, 37(21), 5641-5650.
- (33) Li, X.; Gurzadyan, G. G.; Gelin, M. F.; Domcke, W.; Gong, C.; Liu, J.; Sun, L. Enhanced S<sub>2</sub> Fluorescence from a Free-Base Tetraphenylporphyrin Surface-Mounted Metal Organic Framework. *J. Phys. Chem. C* **2018**, 122(41), 23321-23328.